Supplemental Information for Redox non-innocence and orbital symmetry constraints permit nitrene carbonylation by (dadi)Ti=NAd (Ad = adamantyl)

Spencer P. Heins,[a] Peter T. Wolczanski,*[a] Thomas R. Cundari,*[b] and Samantha N. MacMillan[a]

[a.]Cornell University, Dept. of Chemistry & Chemical Biology, Baker Laboratory, Ithaca, NY, 14853, USA. Email: ptw2@cornell.edu

[b.]University of North Texas, Dept. of Chemistry, CASCaM, Denton, TX, 76201, USA. Email: Thomas.Cundari@unt.edu

Table Of Contents:

I. Experimental Procedures

A. General Considerations:

All manipulations were performed using either glovebox or high vacuum line techniques. All glassware was oven dried. THF and diethyl ether were distilled under nitrogen from purple sodium benzophenone ketyl and vacuum transferred from the same prior to use. Hydrocarbon solvents were treated in the same manner with the addition of 1-2 mL/L tetraglyme. Benzene-d_6 was dried over sodium, vacuum transferred and stored over activated 4Å molecular sieves. THF-d_8 was dried over sodium and stored over purple sodium benzophenone ketyl. Hexamethyldisilazane was purchased from Oakwood Chemicals then dried and stored over activated 4Å molecular sieves. Dimethylphenylphosphine was purchased from Strem Chemicals Inc., degassed and stored in a dry box before use. Nitrous oxide, ferrocene, and 1-azidoadamantane were purchased from Sigma-Aldrich Chemical Company and used as received. N, N'-di-2-(2,6-diisopropylphenylamine)-phenylglyoxaldiimine ($DadiH_2$) was prepared following literature procedures.[1]

NMR spectra were acquired using Mercury 300 MHz, INOVA 400 MHz, or Bruker AV III HD 500 MHz (equipped with a 5 mm BBO Prodigy cryoprobe) spectrometers. Assignments of carbon chemical shifts were determined from HSQCAD and gHMBCAD spectra collected on an INOVA 600 MHz NMR spectrometer. Reaction monitoring for kinetic analysis was performed using an INOVA 600 MHz spectrometer. Chemical shifts are reported relative to benzene-d_6 (^{1}H δ 7.16; ^{13}C{^{1}H} δ 128.06). NMR spectra were processed using MNova 11.0. Infrared spectra were recorded on a 20 Nicolet Avatar 370 DTGX spectrophotometer interfaced to an IBM PC (OMNIC software). Fitting of kinetic data was performed using Igor Pro 6. Heating of NMR tubes to 25, 35, and 45 °C was done using a Hewlett Packard 5890 Series II gas chromatograph oven. Heating of NMR tubes to 55, 65, and 75 °C was done using an oil bath equipped with a Thermo Scientific AC200 immersion circulator.
eneral Procedure for NMR Tube Reactions: Flame-dried NMR

B. Synthetic procedures:

1. *Sodium bis(trimethylsilyl)amide:* This is a modified literature procedure.[2] To a 300 mL round bottom flask charged with NaH (4.21 g, 175.5 mmol) and toluene (150 mL) was added hexamethyldisilazane (40mL, 190.8 mmol) via syringe under argon purge. After heating to reflux for 48 hours, the reaction mixture was concentrated to *ca.* 35 mL and filtered. The filter cake was then washed with toluene (2x) then stripped of all volatiles, then washed again with pentane (3x). Following removal of all volatiles NaHMDS was obtained as a white voluminous powder (16.990 g, 92.5 mmol, 48 %). ^{1}H NMR (C_6D_6, 300MHz, 295K): δ 0.12 (s, 18H).

2. *Titanium-dichloride-bis(tetramethylethylenediamine):* This is a modified literature procedure.[3] In a dry box under a N_2 atmosphere, a 100 mL round bottom flask was charged with $TiCl_3(THF)_3$ (5.00 g, 13.6 mmol) and freshly chopped lithium metal (321 mg, 46.2 mmol). The reaction flask was then assembled onto a large swivel frit with a 100 mL receiving flask. The swivel frit apparatus was degassed then put under an argon atmosphere. Under a strong argon purge, the lithium metal was cut as much as possible using a sharpened spatula. The swivel-frit apparatus was degassed and THF (65 mL) then TMEDA (12 mL, 80.0 mmol) were vac. transferred to the reaction flask. The reaction mixture was allowed to warm to room temperature and stirred for 43 hours. The swivel-frit apparatus was degassed, and the reaction mixture filtered. The filter-cake was washed until no purple solid remained on the fritted filter. The reaction mixture was then concentrated to *ca*. 30 mL and cooled to -78 °C while stirring

for 30 min. The entire frit apparatus was then cooled to -78 °C and the reaction mixture was filtered and washed once with the remaining solvent. All volatiles were removed by vacuum and $TiCl_2(TMEDA)_2$ was collected as a purple crystalline solid (2.952 g, 62 %).

3. *Bis(tetrahydrofuran-2-yl)sodium(III) (((1E,1'E)-ethane-1,2-diylidenebis(azanylylidene))bis(2,1-phenylene))bis((2,6-diisopropylphenyl)amide)*, **(dadi)Na_2**. To a 100 mL round bottom flask charged with dadiH_2 (2.0 g, 3.58 mmol) and NaHMDS (1.313 g, 7.16 mmol) was added 40 mL freshly distilled THF at –78 °C. The reaction was allowed to warm to room temperature over the course of 30 minutes then the reaction volume was concentrated to *ca.* 15 mL. The blue solution was cooled to -78 oC then 40 mL of freshly distilled pentane was added resulting in blue precipitate which was filtered. After removal of all volatiles, Na_2dadi$(THF)_4$ was collected as a blue crystalline solid (2.994 g, 3.36 mmol, 94 %). *Na_2dadi$(THF)_4$* was quenched with a mixture of C_6D_6 and saturated $NH_4Cl_{(aq)}$ to determine the amount of THF in the product. ^{1}H NMR (300 MHz, THF-d_8) δ 1.04 (dd, *J* = 10.9, 6.9 Hz, 24H), 3.39 (hept, *J* = 7.3, 6.9 Hz, 4H), 5.58 (t, J = 7.0 Hz, 2H), 5.67 (d, *J* = 8.4 Hz, 2H), 6.35 (t, J = 7.4 Hz, 2H), 6.72 (t, J = 7.7 Hz, 2H), 6.87 (d, *J* = 7.7 Hz, 2H), 6.94 (d, *J* = 7.4 Hz, 2H), 8.32 (s, 2H). ^{13}C NMR (126 MHz, THF-d_8) δ 24.55, 25.20, 26.55, 68.39, 106.49, 116.53, 117.16, 120.55, 123.57, 129.58, 135.33, 143.42, 148.39, 154.45, 158.47.

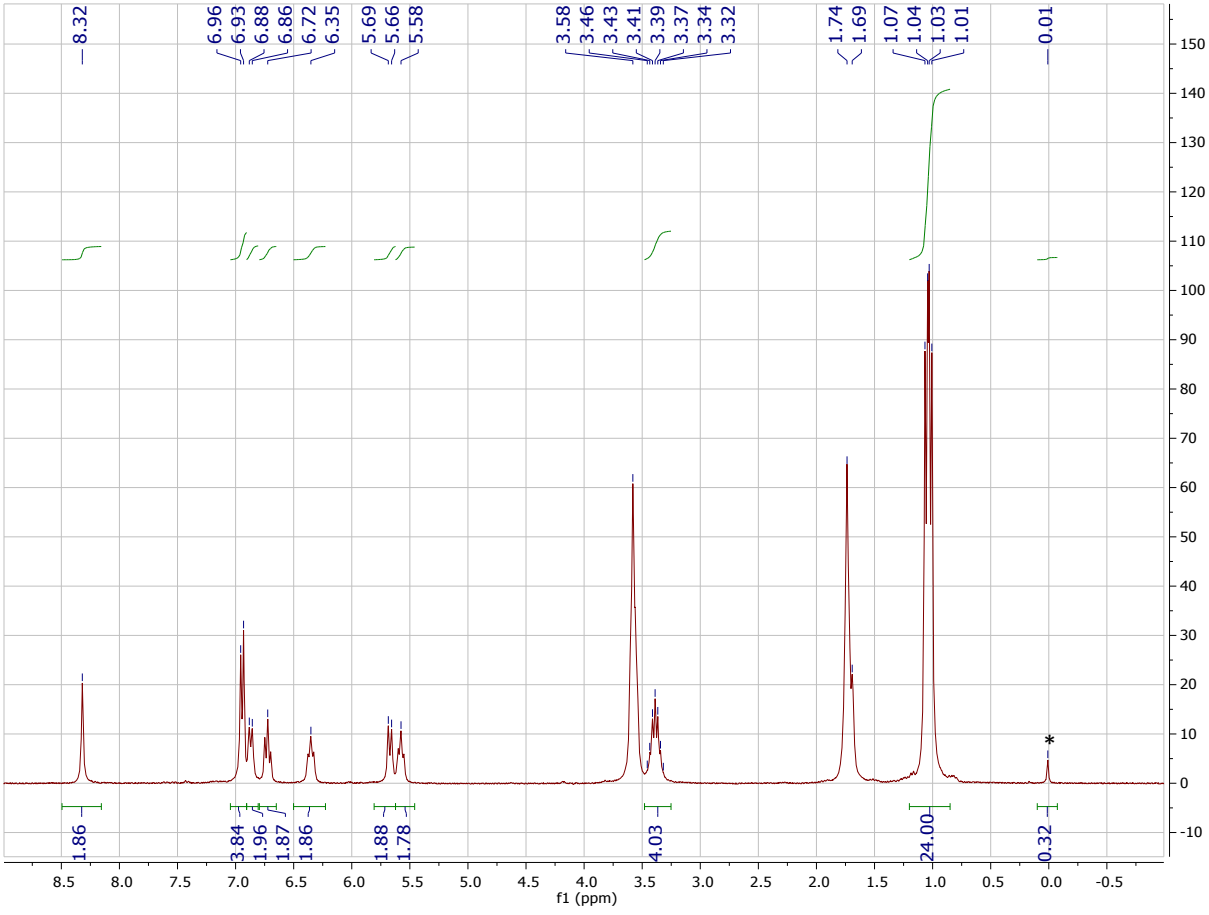

Fig. S1. ^{1}H NMR spectrum of (dadi)Na_2; THF-d_8, 300 MHz, 295K, * = trace hexamethyldisilazane.

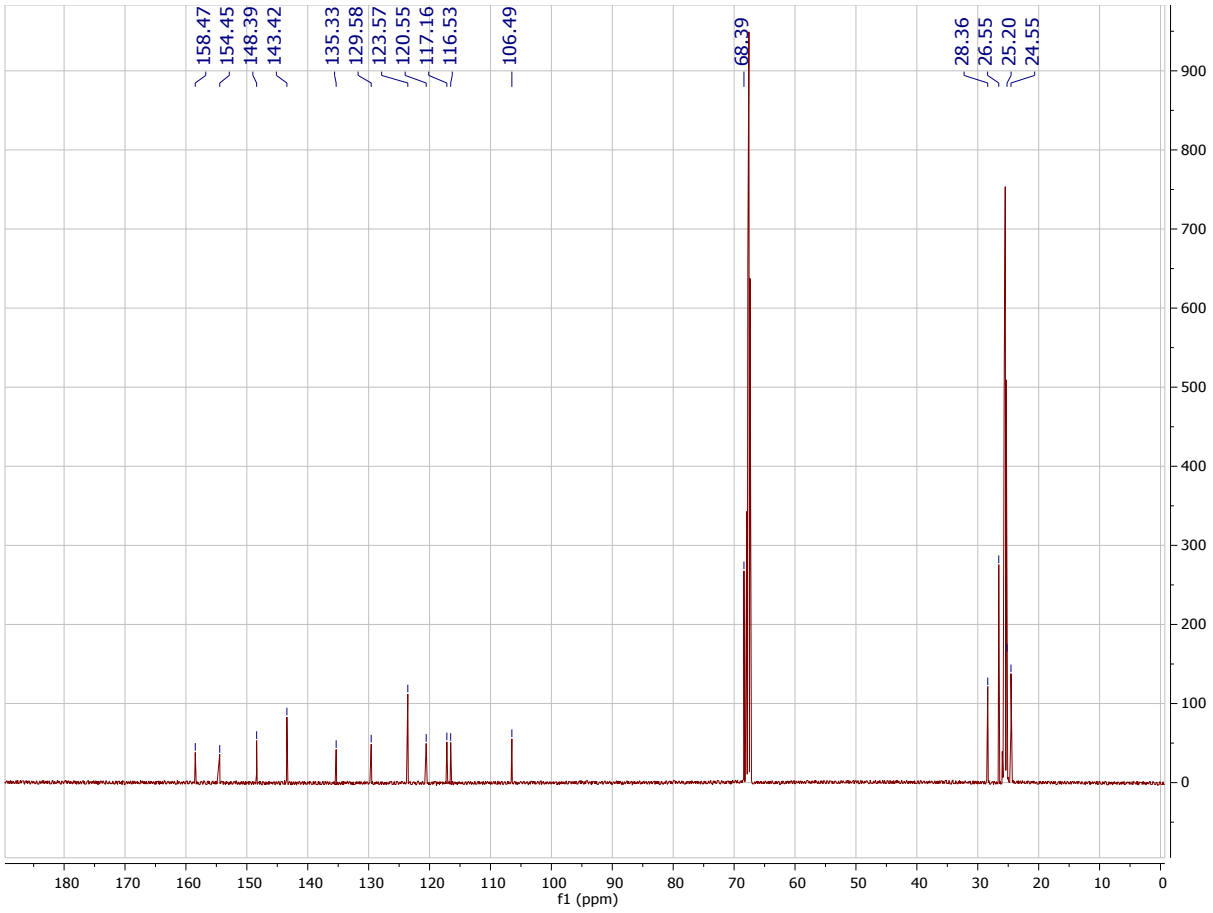

Fig. S2. $^{13}C\{^{1}H\}$ NMR spectrum of (dadi)Na_2; THF-d_8, 126 MHz, 295K.

4. *Titanium N, N'-di-2-(2,6-diisopropylphenylamide)-phenylglyoxaldiimine-tetrahydrofuran*, **(dadi)Ti(THF)** (**1**-THF). To a 100 mL round bottom flask, cooled to -78 °C and charged with Na_2dadi$(THF)_4$ (1.479 g, 1.66 mmol) and $TiCl_2$(TMEDA) (584 mg, 1.66 mmol) was added ca. 75 mL freshly distilled THF. The reaction mixture was warmed to -20 °C and stirred for 4 hours. The resulting green solution was stripped of volatiles, triturated with THF (3x, 20 mL). 30 mL of cyclohexane was added and the reaction was filtered. The filter cake was washed until the filtrate was colorless. The resulting mixture was cooled to 10 °C for 30 minutes then filtered. After all volatiles were removed, Ti(dadi)THF was collected as an olive green powder with 0.66 eq. of residual cyclohexane (597 mg, 48 %). *Varying amounts of cyclohexane were present in the isolated product, ranging from 0.50–1.3 eq. per titanium. ^{1}H NMR (C_6D_6, 400MHz, 295K): δ 0.57 (d, *J* = 6.6 Hz, 6H) , 0.94 (d, *J* = 6.4 Hz, 6H) , 1.06 (d, *J* = 5.9 Hz, 12H) , 1.25 – 1.15 (m, 4H) , 1.40 (s, 4H), 2.48 – 2.29 (m, 2H), 3.50 (p, J= 6.5 Hz, 2H) , 3.89 (t, J= 6.5 Hz, 4H) , 5.78 (d, *J* = 7.8 Hz, 2H) , 6.48 (dd, *J* = 7.7, 0.9 Hz, 2H) , 6.69 – 6.57 (m, 4H) , 6.81 (t, *J* = 7.5 Hz, 2H) , 7.01 (d, *J* = 6.2 Hz, 2H), 7.14 – 7.06 (m, 6H). $^{13}C\{^{1}H\}$ NMR (C_6D_6, 126 MHz, 295K) δ 22.92, 23.54, 24.67, 25.12, 25.67, 26.87, 28.98, 74.42, 105.98, 113.76, 120.41, 123.28, 123.52, 125.27, 126.45, 127.75, 141.77, 143.50, 143.82, 146.25, 151.78.

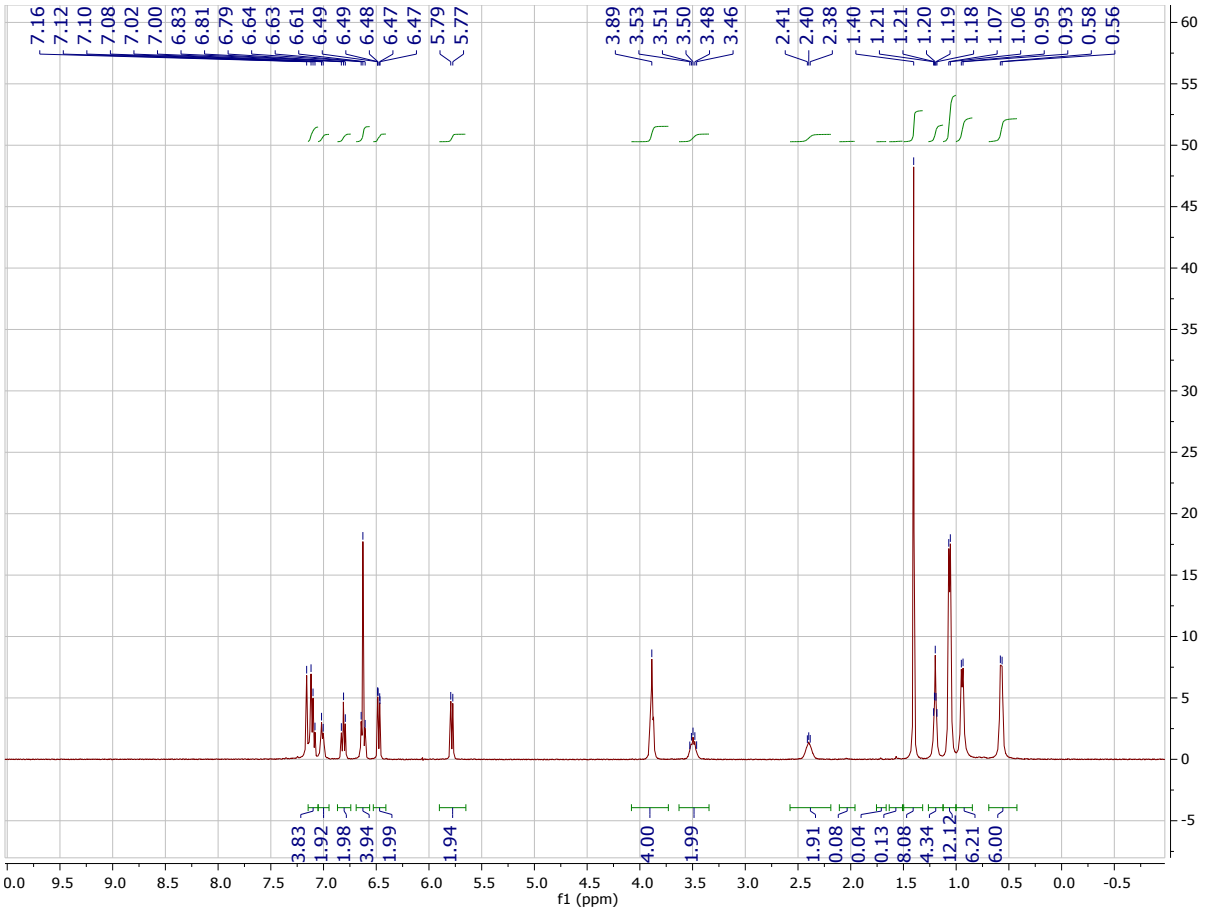

Fig. S3. ^{1}H NMR spectrum of Ti(dadi)THF·^{c}Hex$_{(0.66)}$ (**1**-THF); C_6D_6, 400MHz, 295K.

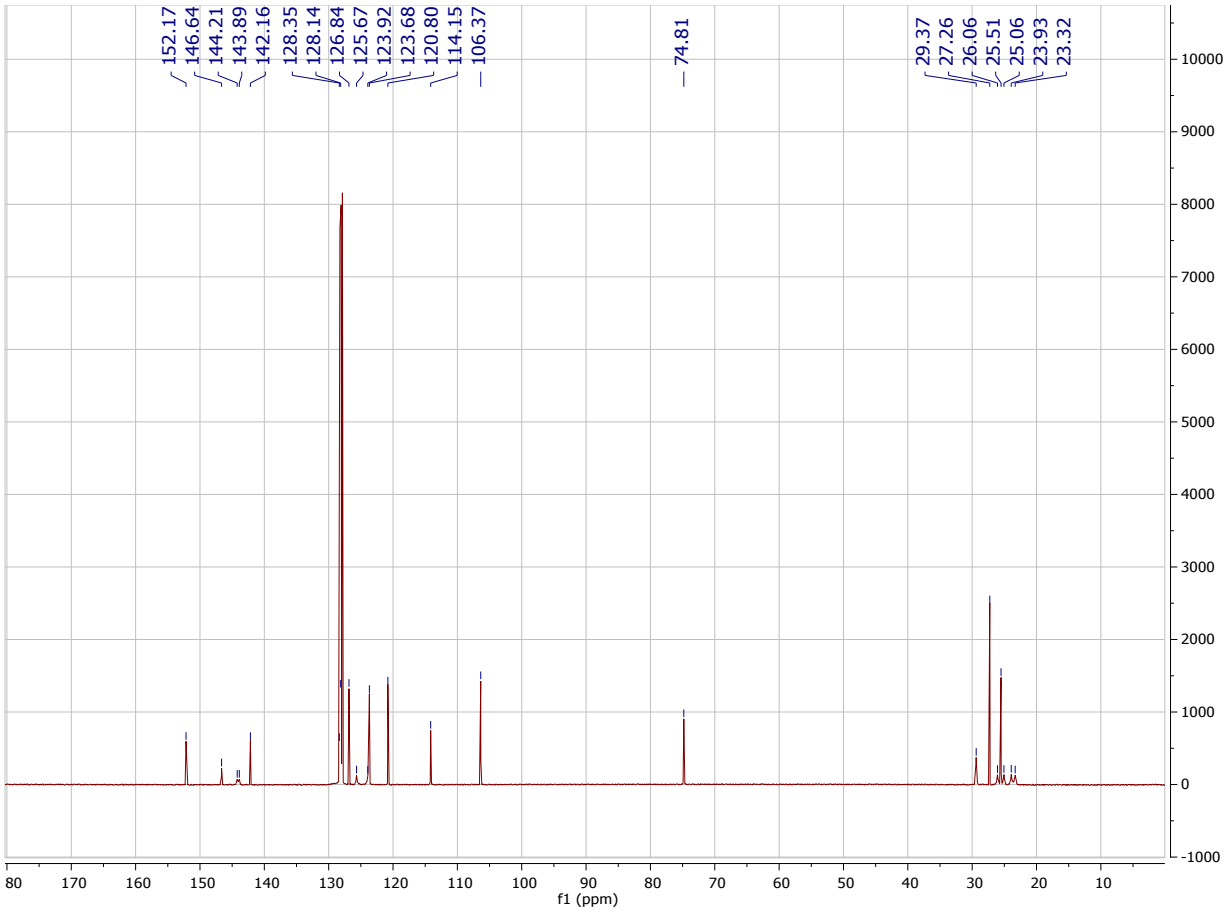

Fig. S4. ^{13}C NMR spectrum of Ti(dadi)THF·^{c}Hex$_{(0.89)}$ (**1**-THF); C_6D_6, 126 MHz, 295 K.

5. *Titanium N, N'-di-2-(2,6-diisopropylphenylamide)-phenylglyoxaldiimine-dimethylphenyphosphine*, **(dadi)TiPMe$_2$Ph** (**1**-PMe$_2$Ph). To a 100 mL round bottom flask, cooled to -78 °C and charged with Na_2dadi (1.000 g, 8.78 mmol) and $TiCl_2$(TMEDA) (584 mg, 1.66 mmol) was added *ca.* 75 mL freshly distilled THF. The reaction mixture was warmed to -20 °C and stirred for 2 hours. The resulting green solution was stripped of volatiles, triturated with THF (3x, ca. 20 mL). 25 mL of freshly distilled benzene was added and the reaction mixture was warmed to 23 °C. Next, a solution of PMe$_2$Ph in 0.7 mL of benzene was added via syringe under an argon purge. The resulting red solution was stirred for 1 hour. The benzene was then removed in *vacuo* and 30 mL of freshly distilled hexanes was added to the reaction flask. The mixture was filtered and the filter cake was washed until colorless. The filtered solution was concentrated to ca. 15 mL total volume, cooled to -78 °C and filtered. After all volatiles were removed, Ti(dadi)PMe$_2$Ph was collected as a maroon solid (706 mg, 0.95 mmol, 57%). A single crystal suitable for X-Ray diffraction was acquired by slow diffusion of hexanes into a concentrated Et_2O solution. ^{1}H NMR (C_6D_6, 500 MHz, 295K) δ 0.40 (d, *J* = 6.8 Hz, 6H, Me), 0.83 (d, *J* = 6.7 Hz, 6H, Me), 1.03-1.06 (m, 12H, Me), 1.21 (d, *J* = 7.8 Hz, 6H), 2.07 (sept, *J* = 6.9 Hz, 2H), 3.74 (sept, *J* = 6.8 Hz, 2H), 5.81 (dd, *J* = 8.0, 1.3 Hz, 2H), 6.41 (dd, *J* = 7.8, 1.3 Hz, 2H), 6.60 (td, *J* = 7.7, 1.3 Hz, 2H), 6.62 (s, 2H), 6.79 (td, *J* = 7.5, 1.3 Hz, 2H), 6.90 – 7.01 (m, 5H), 7.08 (t, *J* = 7.7 Hz, 2H), 7.15 – 7.18 (m, 2H), 7.21 – 7.28 (m, 2H). ^{1}H{^{31}P} NMR (C_6D_6, 400 MHz, 295 K) ^{1}H NMR δ 0.40 (d, *J* = 6.8 Hz, 6H), 0.83 (d, *J* = 6.6 Hz, 6H), 1.03-1.06 (m, 12H), 1.20 (s, 6H), 2.07 (p, *J* = 6.8 Hz, 2H), 3.74 (p, *J* = 6.7 Hz, 2H), 5.81 (dd, *J* = 7.9, 1.3 Hz, 2H), 6.41 (dd, *J* = 7.8, 1.3 Hz, 2H), 6.55 – 6.64 (m, 4H), 6.79 (td, *J* = 7.5, 1.3 Hz, 2H), 6.89 – 7.03 (m, 5H), 7.08 (t, *J* = 7.6 Hz, 2H), 7.12 – 7.20 (m, 2H), 7.25 (d, *J* = 7.4 Hz, 2H). ^{31}P NMR (C_6D_6, 202 MHz, 295K) δ -6.40 (s).

$^{13}C\{^{1}H\}$ NMR (C_6D_6, 126 MHz, 295K) δ 10.68 (P-CH_3,d, J_{PC} = 19.1 Hz), 23.42 (^{i}Pr-CH_3), 24.38 (^{i}Pr-CH_3), 25.08 (^{i}Pr-CH_3), 26.26 (^{i}Pr-CH_3), 29.21 (^{i}Pr-CH), 29.60 (^{i}Pr-CH), 107.16 (Ar-CH), 115.36 (Ar-CH), 120.70 (Ar-CH), 123.74 ($^{2,6\text{-iPr}}$Ar-CH), 124.07 (Ar-CH), 125.81 ($^{2,6\text{-iPr}}$Ar-CH), 126.50 ($^{2,6\text{-iPr}}$Ar-CH), 128.92 (Ar-CN), 129.04 (d, J_{PC}=9.3 Hz, P-Ar-CH), 130.19 (d, J_{PC}= 1.4 Hz, P-Ar-CH), 130.83 (d, J_{PC}= 11.8 Hz, P-Ar-CH), 133.72 (d, J_{PC}= 31.5 Hz, P-Ar-C) 142.10 (d, J_{PC}= 1.1 Hz, Ar-CN), 143.75 ($^{2,6\text{-iPr}}$Ar-C), 143.84 ($^{2,6\text{-iPr}}$Ar-C), 147.86 ($^{2,6\text{-iPr}}$Ar-CN), 153.30 (Ar-CN).

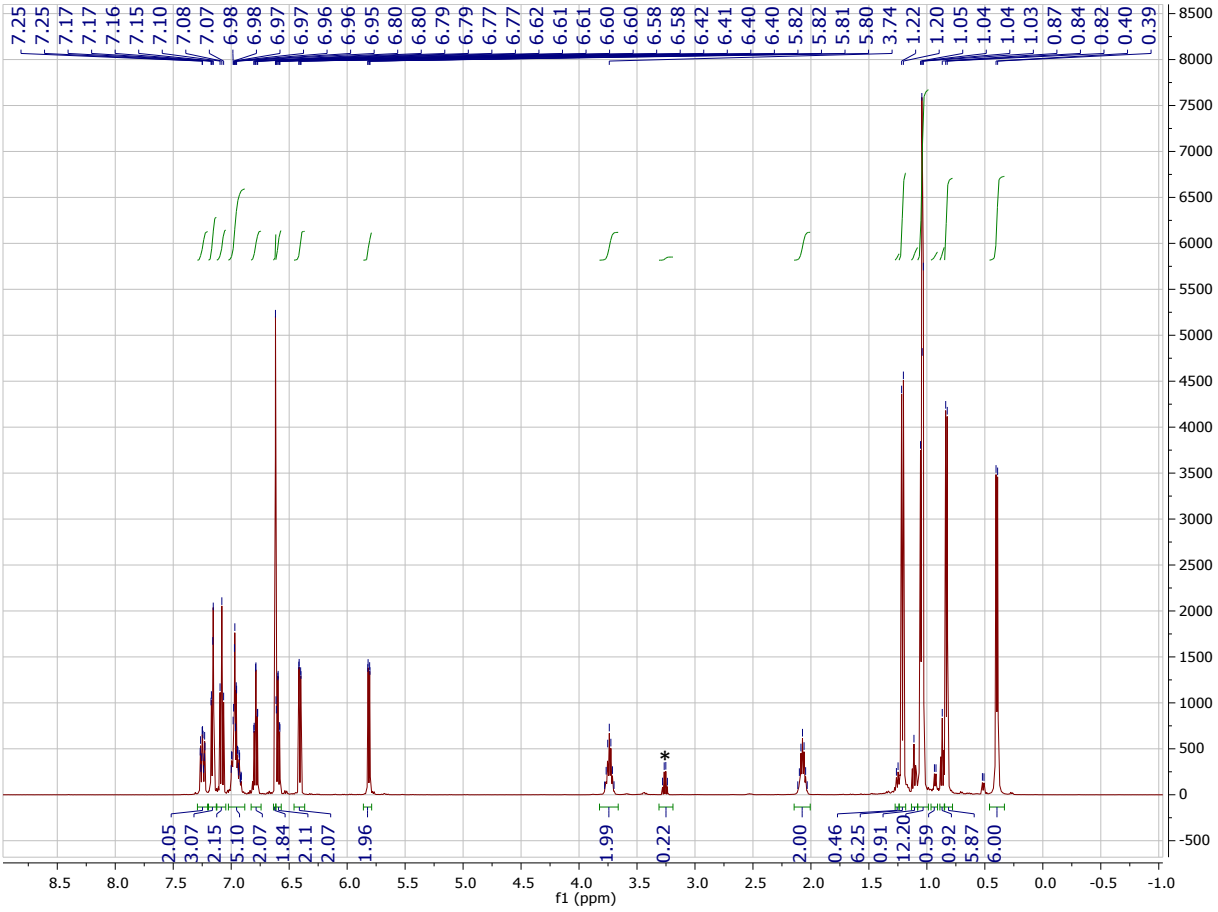

Fig. S5. ^{1}H NMR spectrum of Ti(dadi)PMe_2Ph (**1**-PMe_2Ph); C_6D_6, 500 MHz, 295K, * = trace Et_2O.

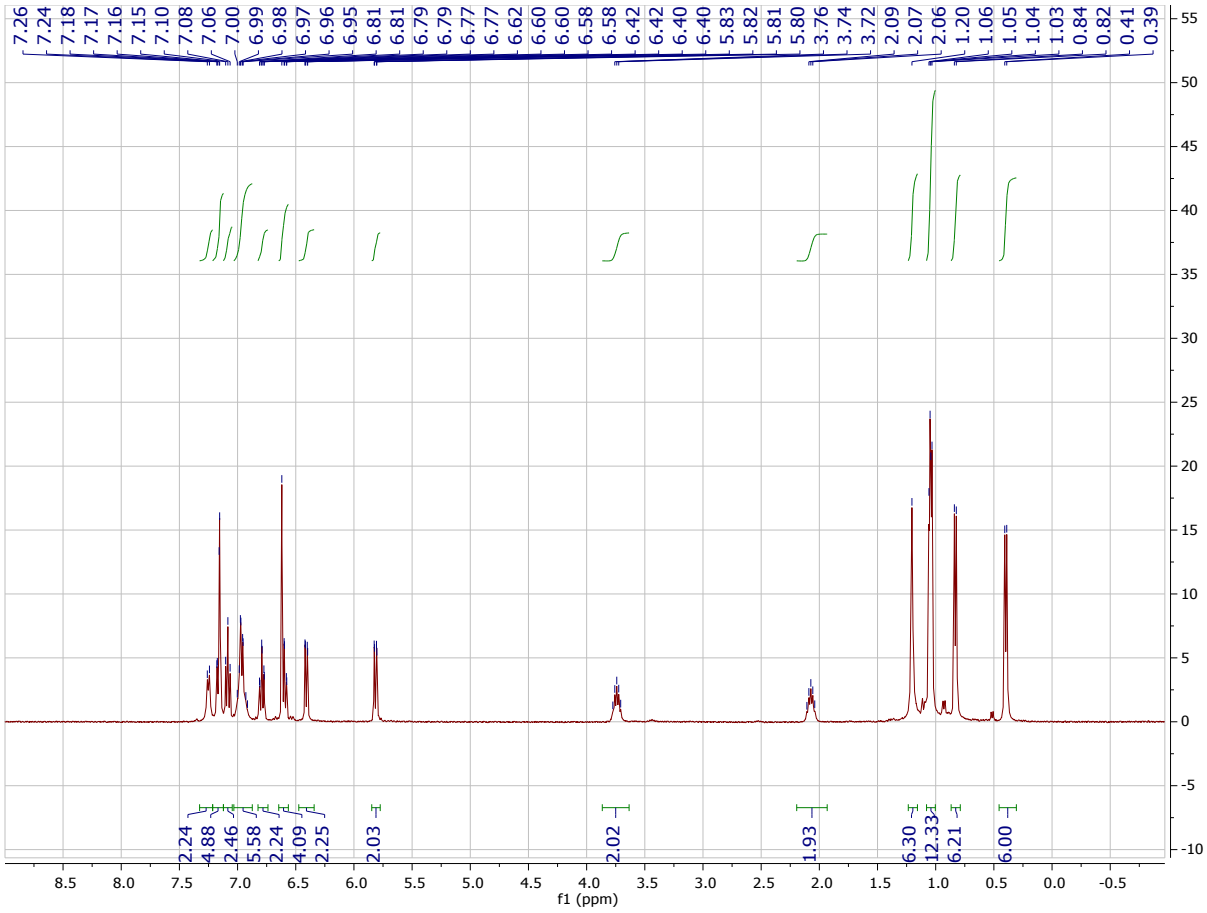

Fig. S6. $^{1}H\{^{31}P\}$ NMR spectrum of Ti(dadi)PMe_2Ph (**1**-PMe_2Ph); C_6D_6, 400 MHz, 295K.

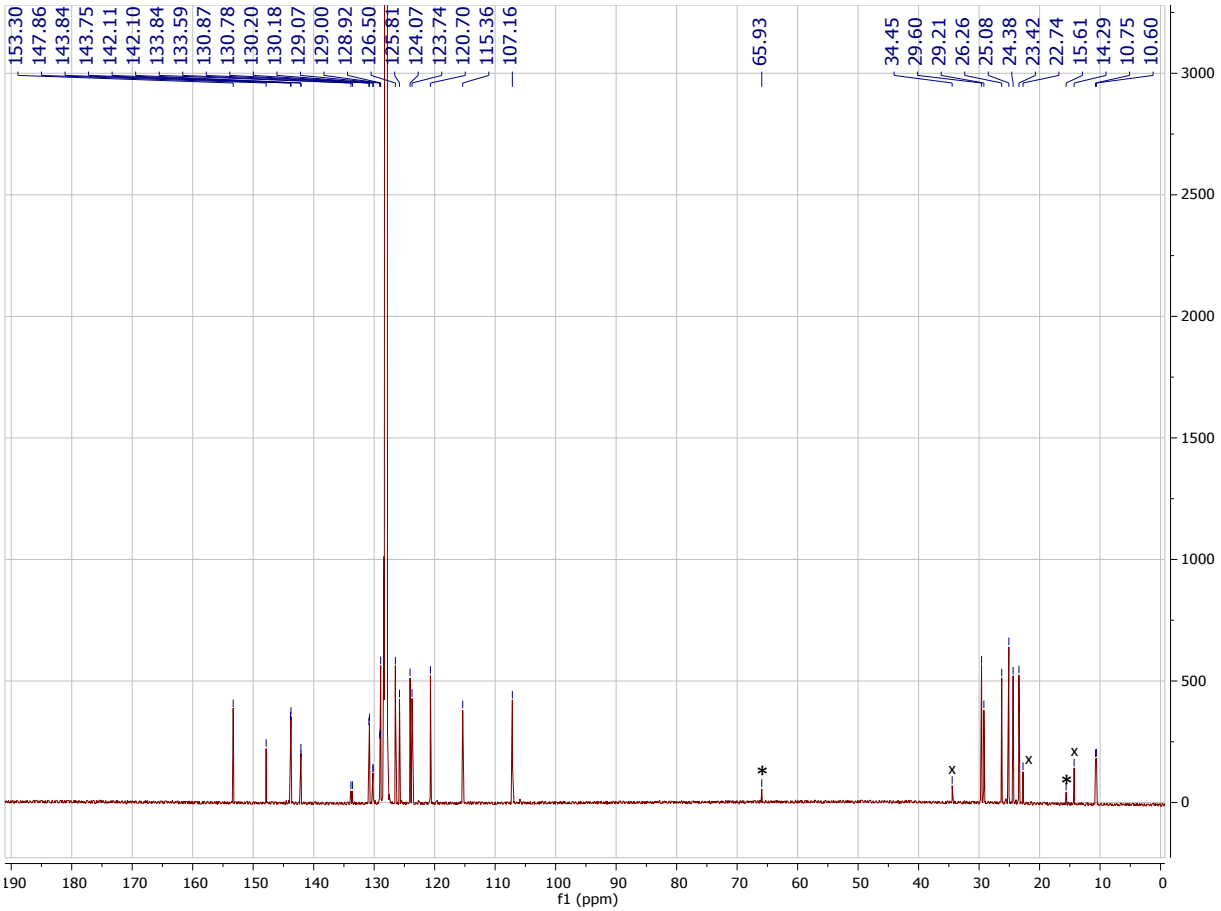

Fig. S7. $^{13}C\{^{1}H\}$ NMR spectrum of Ti(dadi)PMe_2Ph (**1**-PMe_2Ph); C_6D_6, 126 MHz, 295K, * = trace Et_2O, ^{x} = trace impurities.

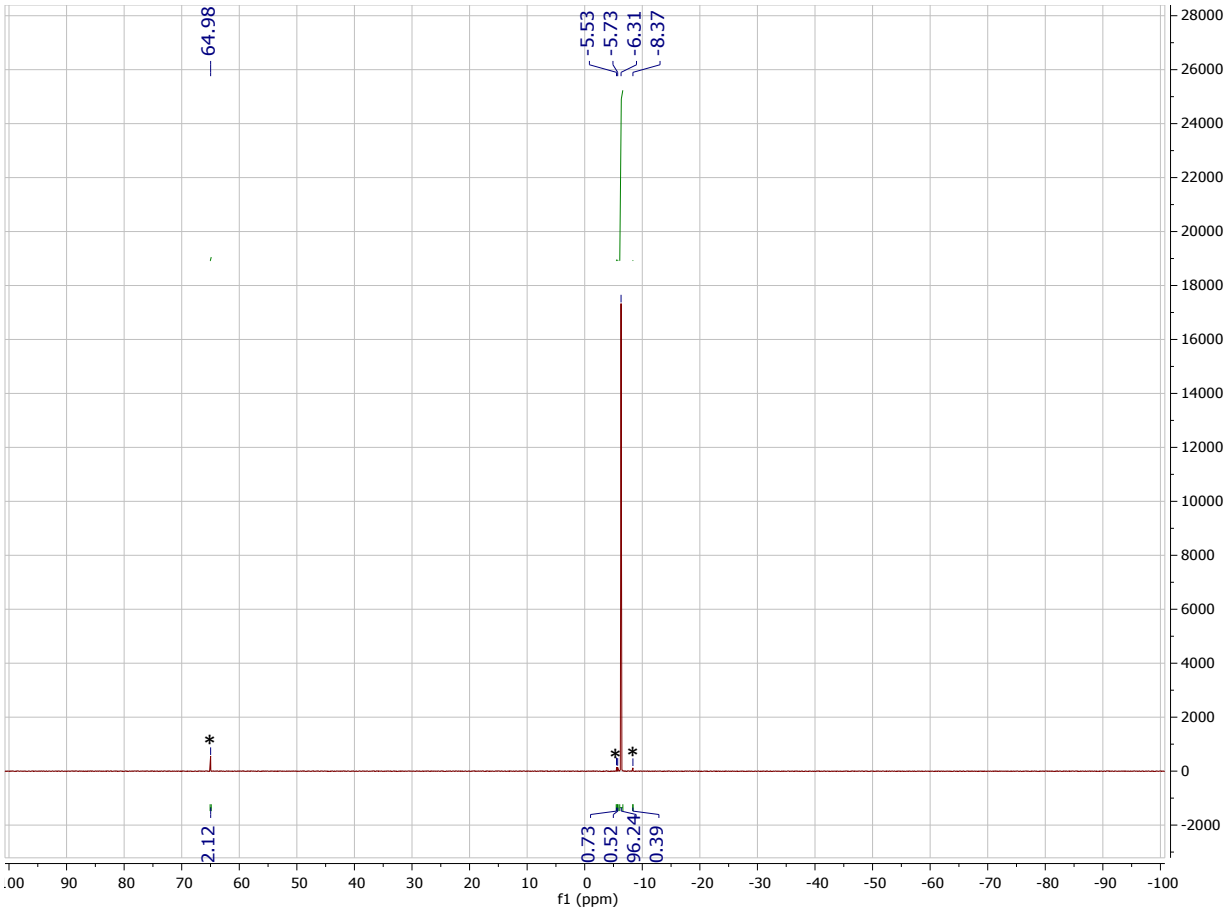

Fig. S8. ^{31}P NMR spectrum of Ti(dadi)PMe_2Ph (**1**-PMe_2Ph); C_6D_6, 202 MHz, 295K, * = trace impurities.

6. *Titanium N, N'-di-2-(2,6-diisopropylphenylamide)-phenylglyoxaldiimine-1-imidoadamantane*, **(dadi)Ti=NAd** (**2**=NAd). To a 50 mL round bottom flask charged with Ti(dadi)THF·$^{c}Hex_{(0.89)}$ (317 mg,0.42 mmol) and C_6H_6 (1.9 mL) was added a solution of 1-azidoadamantane (74 mg, 0.42 mmol) in 1.1 mL of C_6H_6. Effervescence and an immediate color change to red were observed. The reaction solution was stirred for 15 minutes at room temperature then attached to a swivel frit. The crude mixture was triturated with hexanes (5x, 15 mL). The red solid was taken up in hexanes (*ca.* 30 mL), cooled to -78 °C and filtered. The red filter cake was washed two times with hexanes and then all volatiles were removed by vacuum. Ti(dadi)NAd was collected as a maroon red powder (236 mg, 0.31 mmol, 74 %). ^1H NMR (C_6D_6, 400 MHz, 295K) δ 0.87 (d, *J* = 6.8 Hz, 6H), 1.10 (d, *J* = 4.9 Hz, 6H), 1.11 (d, *J* = 5.2 Hz, 6H), 1.39 (d, *J* = 6.6 Hz, 6H), 1.50 (q, *J* = 12.3 Hz, 6H), 1.93 (s, 3H), 1.99 (s, 6H), 3.19 (p, *J* = 6.8 Hz, 2H), 4.15 (sept, *J* = 6.8 Hz, 2H), 5.71 (d, *J* = 8.4 Hz, 2H), 6.07 (t, *J* = 7.4 Hz, 2H), 6.30 (s, 2H), 6.42 (d, *J* = 8.1 Hz, 2H), 6.46 (t, *J* = 7.7 Hz, 2H), 7.07 – 7.14 (m, 3H), 7.17 (td, *J* = 8.4, 7.9, 2.0 Hz, 3H). $^{13}C\{^1H\}$ NMR (C_6D_6, 126 MHz, 295K) δ 23.93, 24.18, 24.42, 26.51, 29.15, 29.44, 30.32, 36.88, 45.42, 72.71, 115.73, 116.54, 118.55, 124.68, 124.92, 125.60, 133.46, 134.34, 141.04, 144.82, 146.03, 146.06, 164.10.

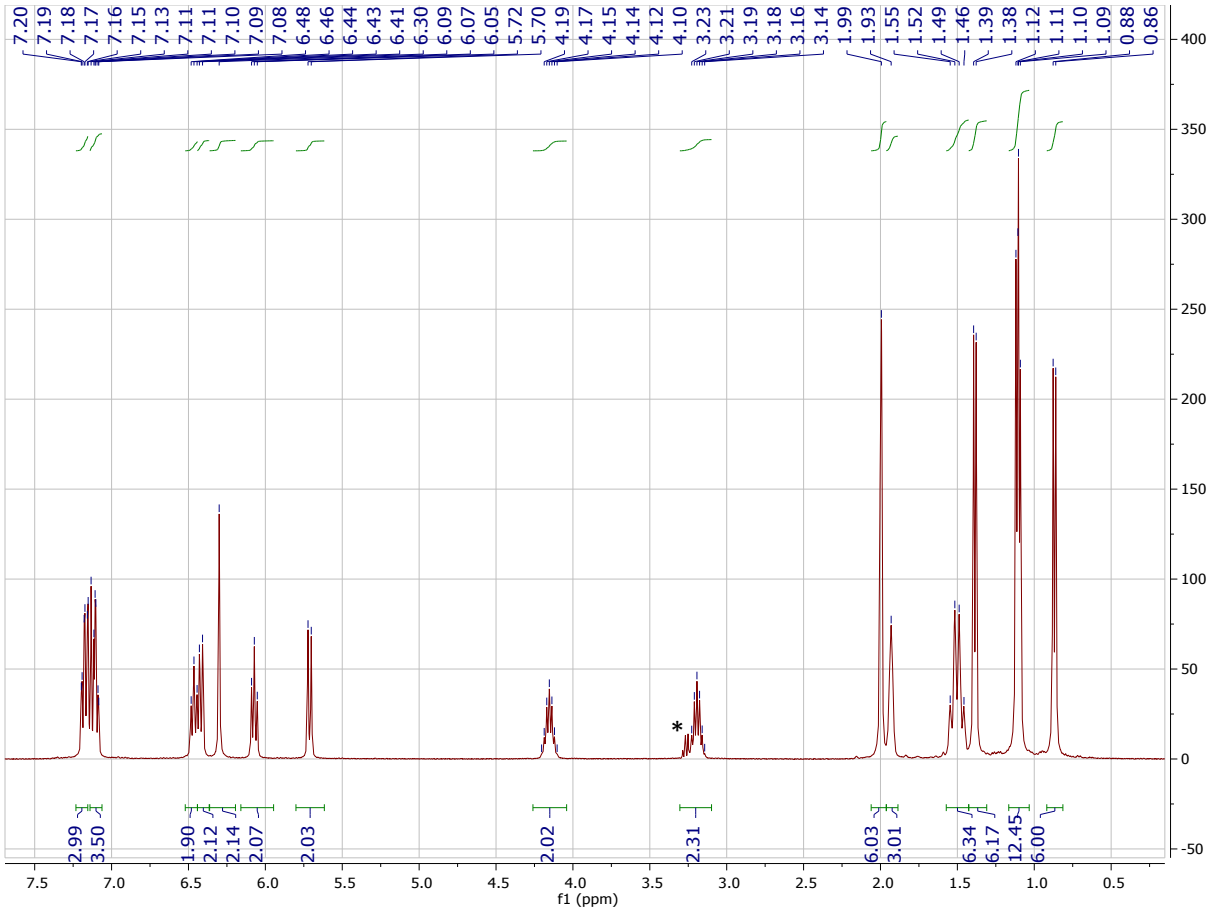

Fig. S9. ^{1}H NMR spectrum of Ti(dadi)NAd (**2**=Ad); C_6D_6, 400 MHz, 295K, * = trace Et_2O.

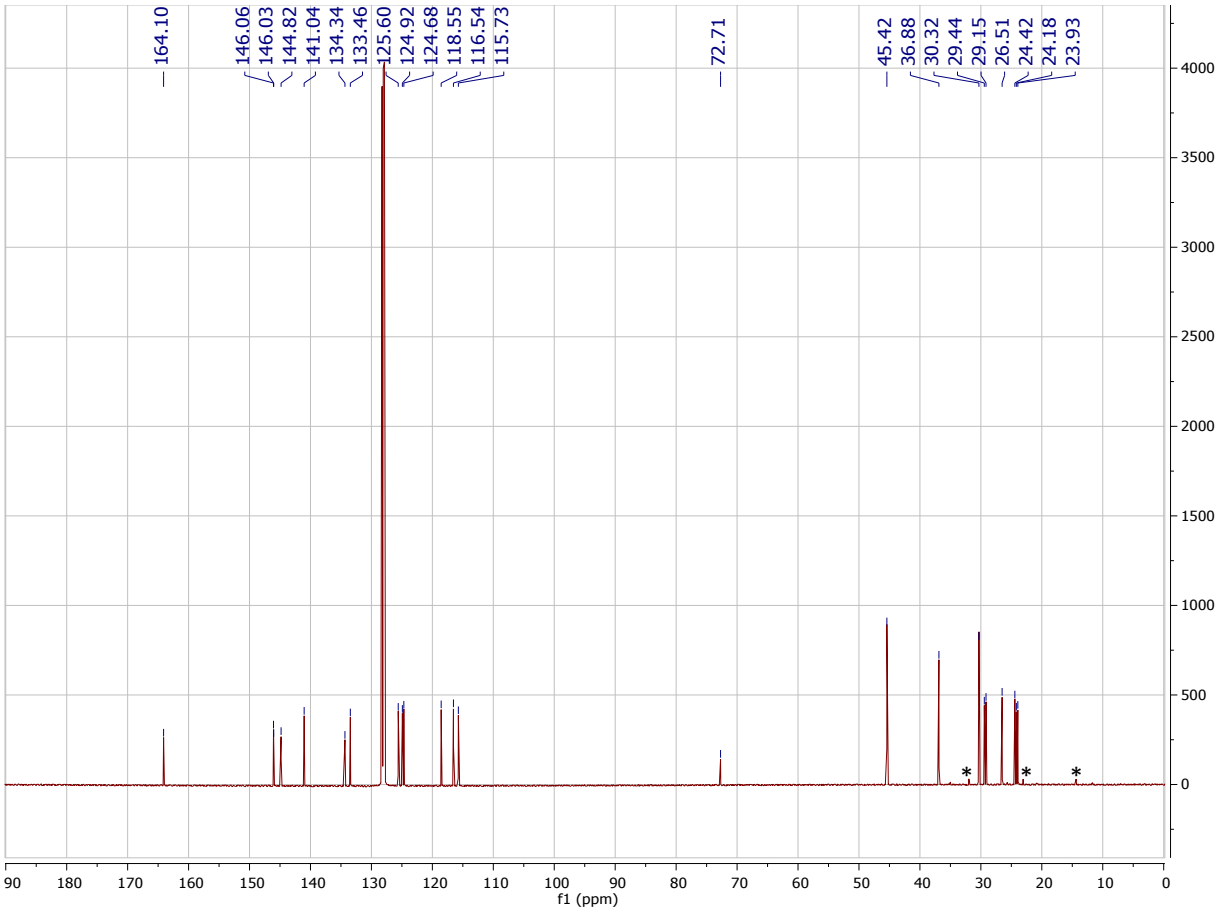

Fig. S10. $^{13}C\{^{1}H\}$ NMR spectrum of Ti(dadi)NAd (**2**=Ad); C_6D_6, 126 MHz, 295K. * = impurities

7. *Titanium N, N'-di-2-(2,6-diisopropylphenylamide)-phenylglyoxaldiimine-oxide*, **(dadi)Ti=O** (**2**=O). A 50 mL round bottom flask attached to a small swivel frit was charged with Ti(dadi)THF·$^{c}Hex_{(1.3)}$ (202 mg, 0.256 mmol). To this flask was added *ca.* 20 mL of freshly distilled benzene. Upon thawing and warming to room temperature, the reaction apparatus was placed under 1 atmosphere of $N_2O_{(g)}$ and purged for 60 seconds while stirring vigorously, then the needle valve was closed. The reaction was stirred at room temperature for 35 minutes, after which the volatiles were pumped away and the reaction solution was concentrated to approximately 1 mL. The resulting mixture was filtered and the filter-cake was washed with benzene (2x) and the remaining volatiles were removed in *vacuo*. 10 mL of pentane was added to the reaction apparatus, the filter-cake was then washed with pentane (3x), followed by removal of the solvent by vacuum. Ti(dadi)O was collected as a lime green powder (115 mg, 0.185 mmol, 70%). A single crystal suitable for X-Ray diffraction was acquired from a concentrated benzene solution of Ti(dadi)O layered with pentane. ^{1}H NMR ^{1}H NMR (C_6D_6, 400 MHz, 295K) δ 0.82 (d, *J* = 6.8 Hz, 6H), 1.06 (d, *J* = 6.8 Hz, 6H), 1.12 (d, *J* = 6.6 Hz, 6H), 1.28 (d, *J* = 6.8 Hz, 6H), 3.04 (p, *J* = 6.8 Hz, 2H), 4.54 (p, *J* = 6.8 Hz, 2H), 5.86 (d, *J* = 8.3 Hz, 2H), 6.16 (ddd, *J* = 8.2, 6.9, 1.2 Hz, 2H), 6.54 – 6.62 (m, 4H), 6.66 (s, 2H), 7.10 (dd, *J* = 7.5, 1.4 Hz, 2H), 7.20 (d, *J* = 7.6 Hz, 2H), 7.25 (dd, *J* = 7.7, 1.4 Hz, 2H).$^{13}C\{^{1}H\}$ NMR (C_6D_6, 126 MHz, 295K) δ 23.14, 23.53, 24.20, 25.27, 28.86, 28.97, 116.75, 116.92, 117.90, 124.07, 125.26, 126.34, 132.91, 133.51, 143.24, 143.51, 144.84, 147.06.

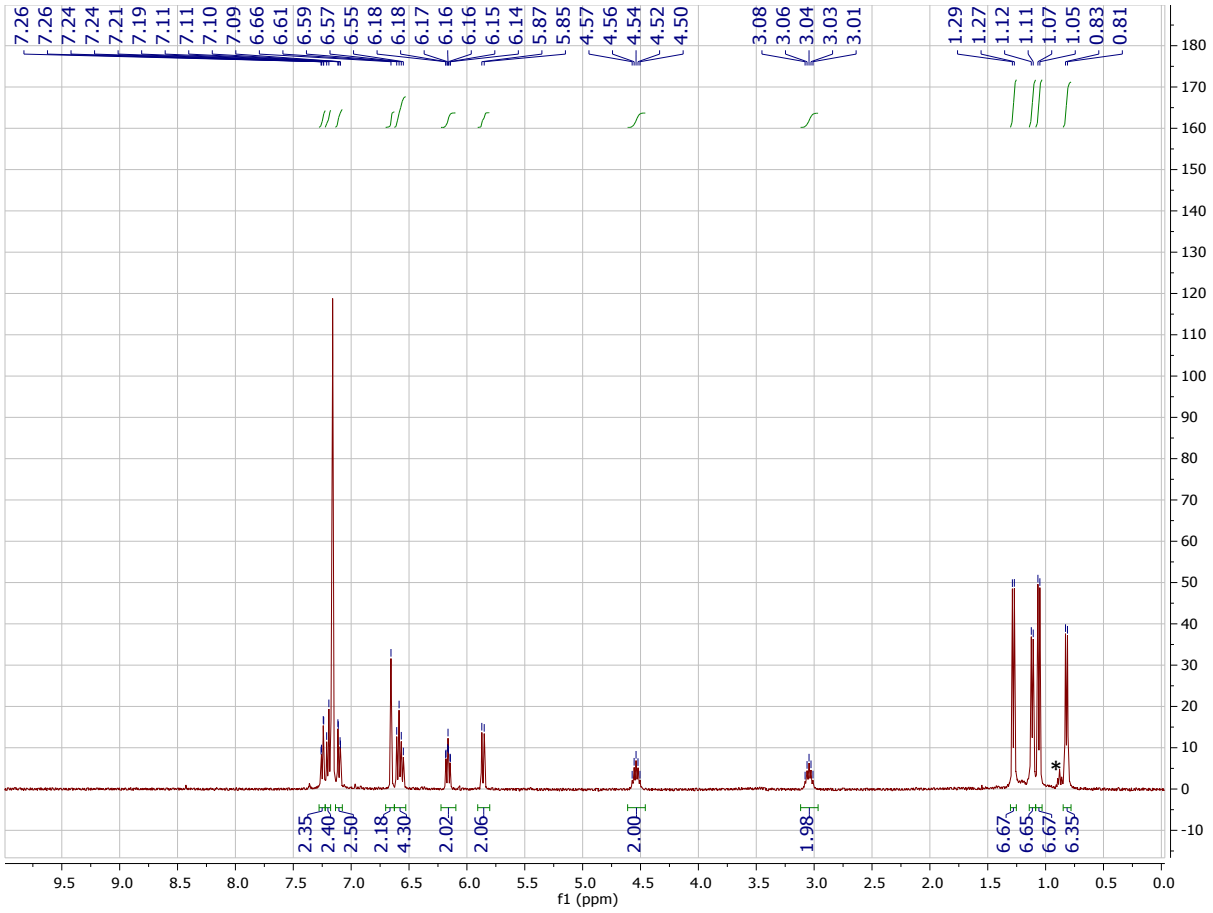

Fig. S11. ^{1}H NMR spectrum of Ti(dadi)O (**2**=O); C_6D_6, 400 MHz, 295K.* = trace pentane

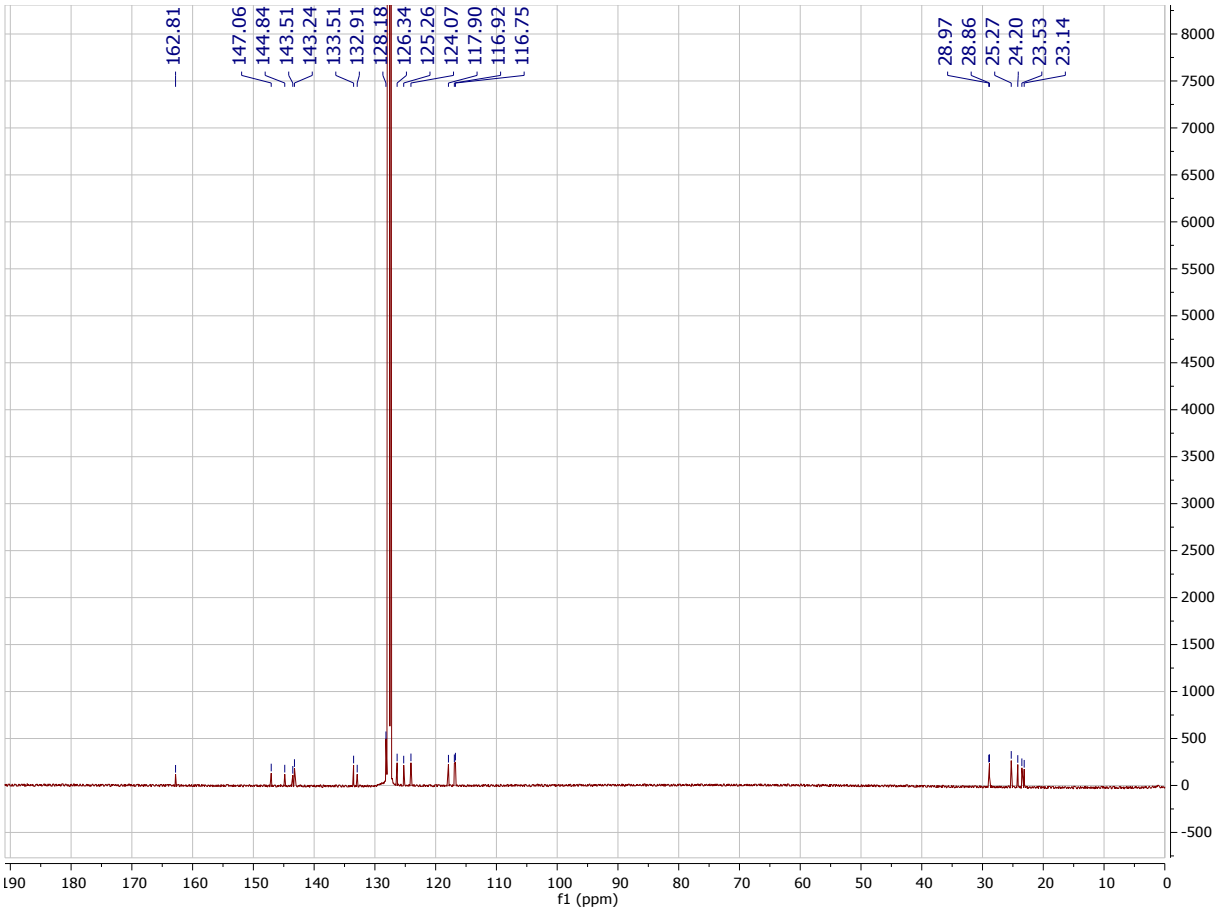

Fig. S12. $^{13}C\{^{1}H\}$ NMR spectrum of Ti(dadi)O (**2**=O); C_6D_6, 126 MHz, 295K.

8. *Titanium N, N'-di-2-(2,6-diisopropylphenylamide)-phenylglyoxaldiimine-bis(methylisocyanide)*, **(dadi)Ti(CNMe)$_2$** (**1**-$(CNMe)_2$). To a 50 mL round bottom flask charged with Ti(dadi)THF·$^{c}Hex_{(0.74)}$ (194 mg, 0.261 mmol) was distilled C_6H_6 (*ca.* 15 mL). An excess of CNMe (*ca.* 8 equivalents) was then condensed into the reaction flask at -78 °C. Upon thawing an immediate color change to blood red was observed. The reaction was stirred for 16 hours then all volatiles were removed in *vacuo* yielding Ti(dadi)$(CNMe)_2$ as a dark red powder (149 mg, 0.216 mmol, 83%). A single crystal suitable for X-Ray diffraction was acquired by diffusion of pentane into a concentrated benzene solution of Ti(dadi)$(CNMe)_2$. ^{1}H NMR (C_6D_6, 300 MHz, 295K) δ 0.79 (d, *J* = 6.8 Hz, 12H), 1.19 (d, *J* = 6.6 Hz, 12H), 2.22 (s, 6H), 3.12 (p, *J* = 6.6 Hz, 4H), 5.79 (dd, *J* = 7.7, 1.5 Hz, 2H), 6.16 (s, 2H), 6.25 (dd, *J* = 7.5, 1.6 Hz, 2H), 6.52 (td, *J* = 7.5, 1.5 Hz, 2H), 6.59 (td, *J* = 7.4, 1.5 Hz, 2H), 7.02 – 7.12 (m, 6H). ^{13}C NMR (C_6D_6, 126 MHz, 295K) δ 23.70 (^{i}Pr-CH_3), 25.49 (^{i}Pr-CH_3), 28.50 (CN-CH_3), 29.45 (^{i}Pr-CH), 105.25 (Ar-CH), 112.88 (Ar-CH), 117.48 (Ar-CH), 124.42 (Ar-CH), 124.73 ($^{2,6\text{-}iPr}$Ar-CH), 125.53 (im-CH), 125.56 ($^{2,6\text{-}iPr}$Ar-CH), 140.58 (Ar-CN), 144.55 ($^{2,6\text{-}iPr}$Ar-C), 146.69 ($^{2,6\text{-}iPr}$Ar-C), 157.61 (Ar-CN), 164.50 (Ti-CNMe). IR (nujol mull, cm^{-1}) 570.89, 615.14, 674.98, 684.25, 710.54, 734.10, 758.48, 793.57, 833.90, 840.32, 868.63, 893.97, 898.85, 939.17, 943.46, 1036.95, 1054.92, 1100.83, 1113.56, 1170.92, 1269.29, 1318.23, 1359.08, 1379.90, 1587.47, 2166.19, 2199.25 (C N), 2222.95, 2642.73, 2704.96, 2719.69, 2751.81, 2932.03, 3056.35.

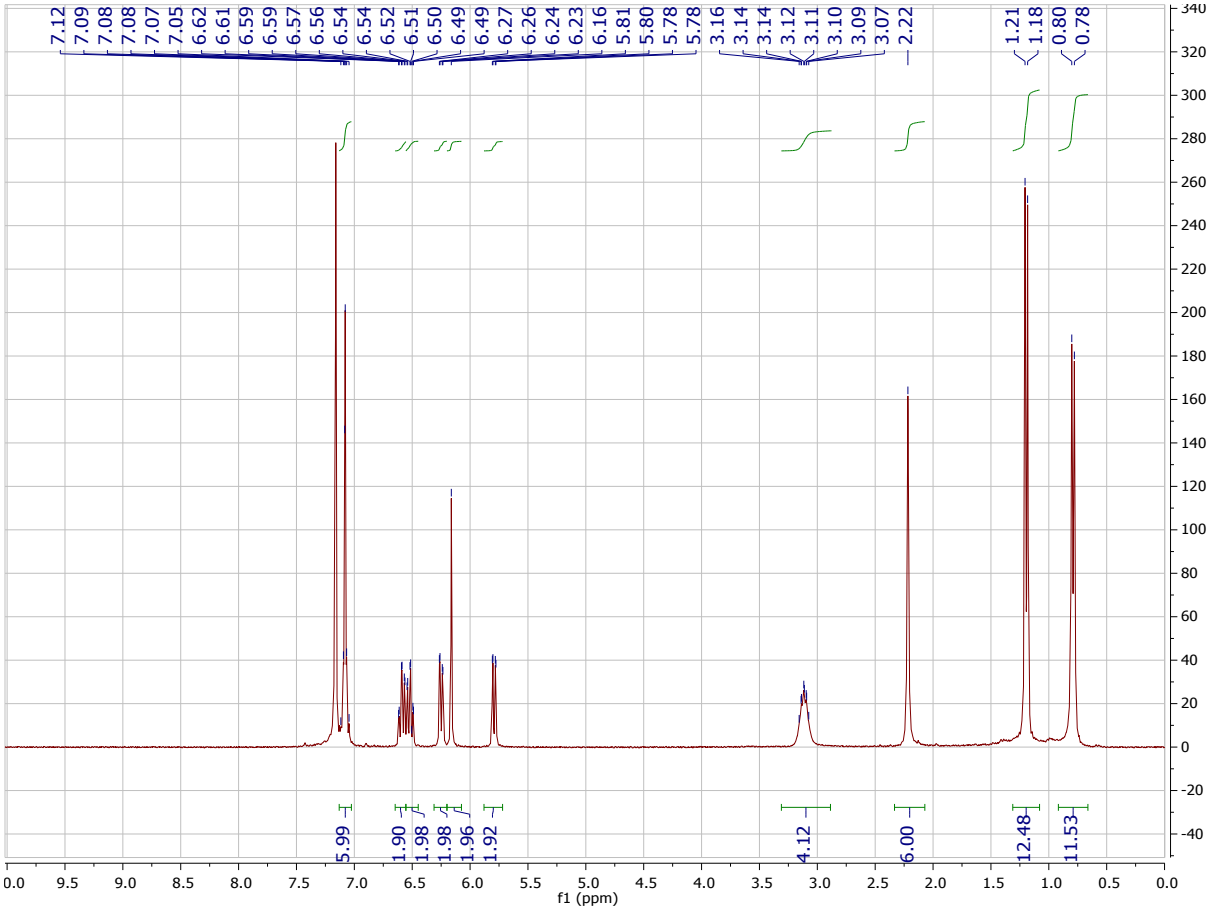

Fig. S13. ^{1}H NMR spectrum of Ti(dadi)$(CNMe)_2$ (**1**-$(CNMe)_2$); C_6D_6, 300 MHz, 295K.

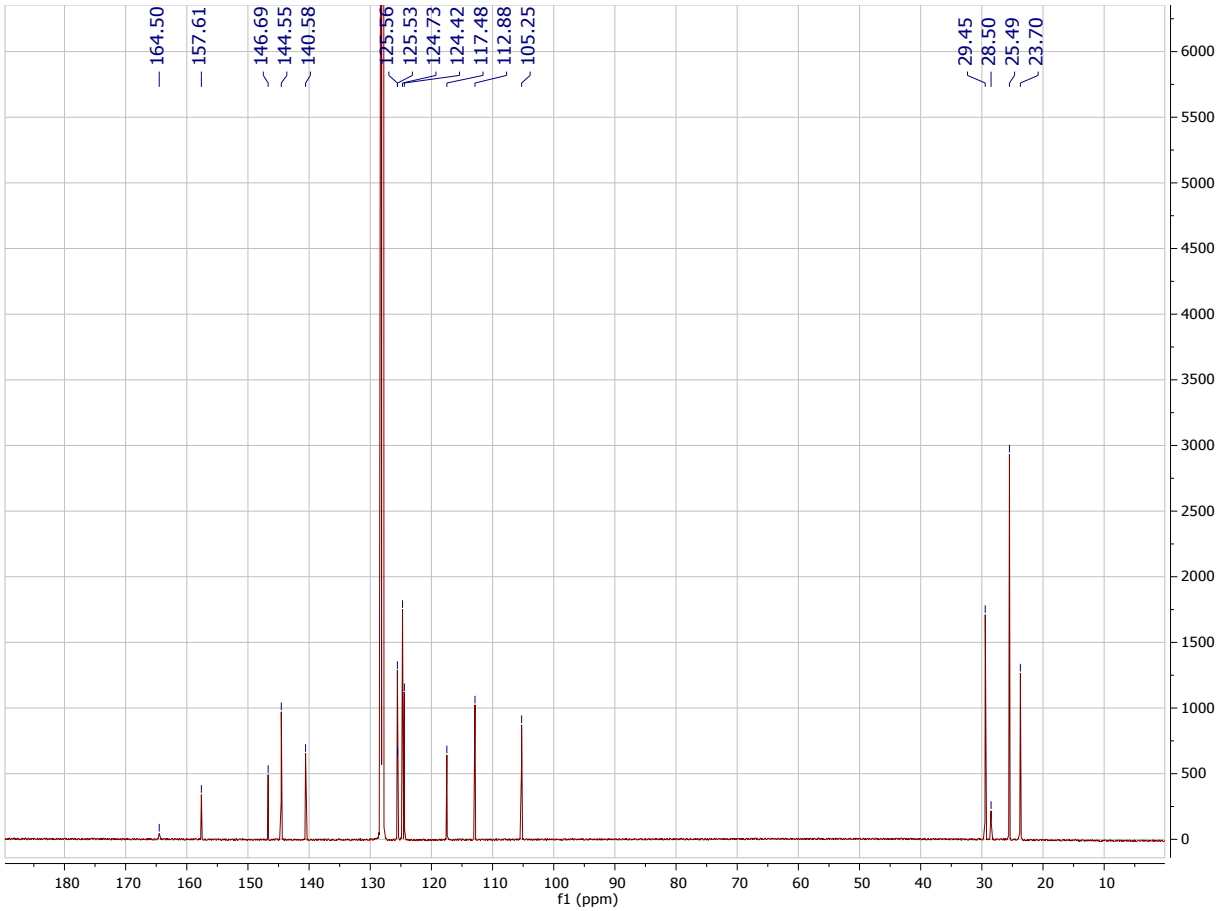

Fig. S14. $^{13}C\{^{1}H\}$ NMR spectrum of Ti(dadi)$(CNMe)_2$ (**1**-$(CNMe)_2$); C_6D_6, 126 MHz, 295K.

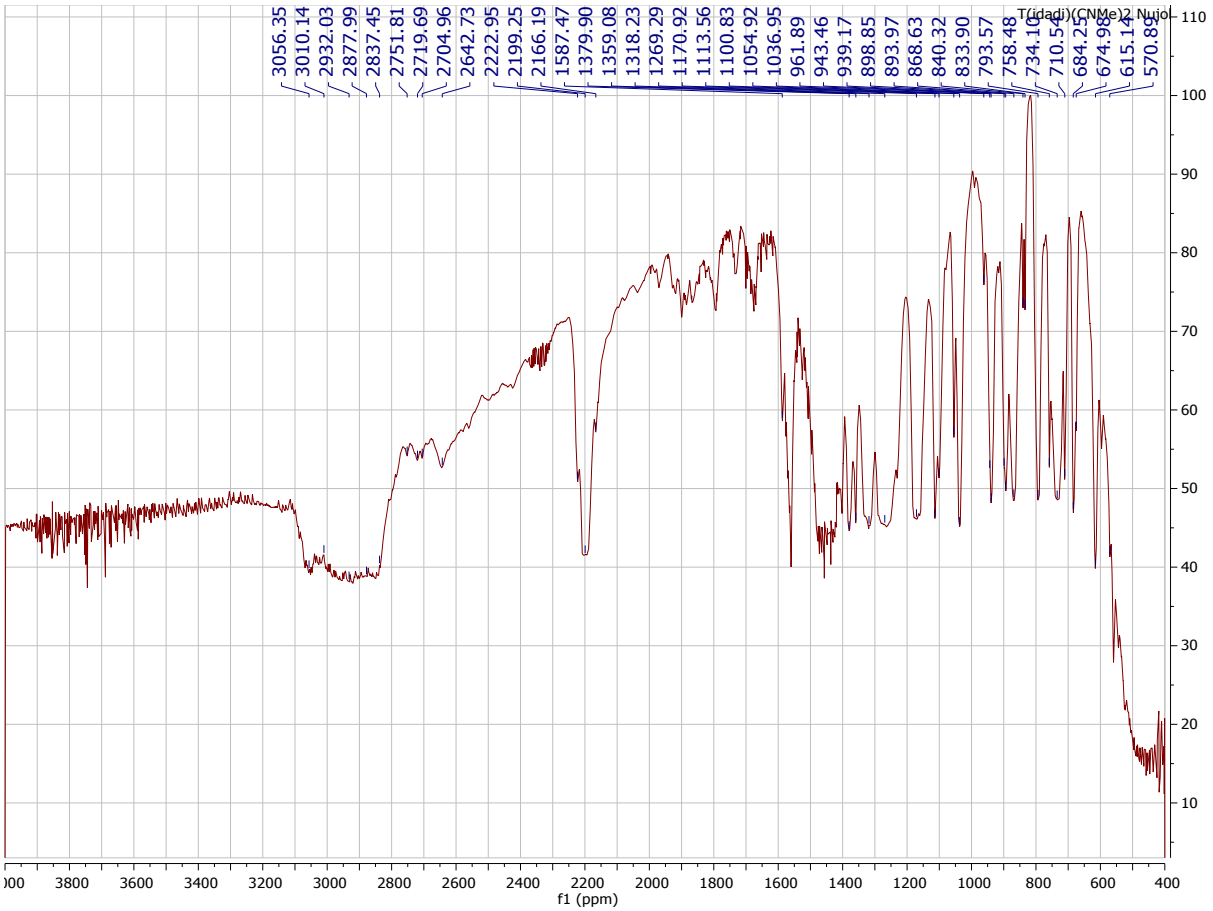

Fig. S15. IR spectrum of Ti(dadi)$(CNMe)_2$ in nujol mull.

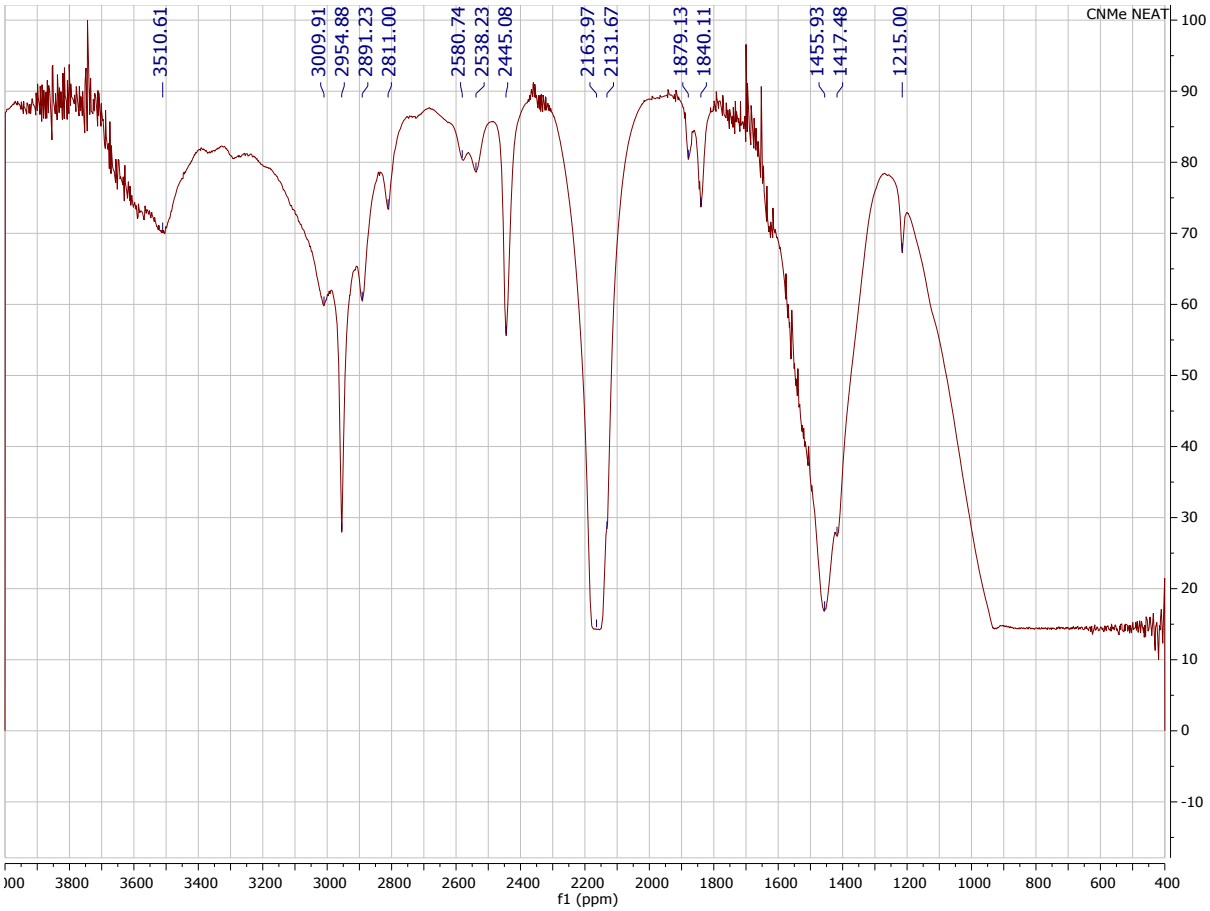

Fig. S16. IR spectrum of NEAT CNMe.

9. *Titanium N, N'-di-2-(2,6-diisopropylphenylamide)-phenylglyoxaldiimine-trimethylphosphineoxide*, **(dadi)Ti-OPMe$_3$** (**1**-OPMe$_3$). To a 25 mL round bottom flask charged with Ti(dadi)O (111 mg, 0.179 mmol) and equipped with a 109 mL gas bulb was distilled C_6H_6 (10 mL). PMe_3 (15 cm Hg, 0.895 mmol) was frozen into the reaction flask then the gas bulb was sealed. Once thawed, the reaction mixture was stirred at room temperature for 72 hours. The volatiles were removed under vacuum yielding Ti(dadi)OPMe$_3$ as a rifle-green crystalline solid (101 mg, 0.106 mmol, 81 %) ^{1}H NMR (400 MHz, Benzene-d_6) ^{1}H NMR (C_6D_6, 400 MHz, 295K) δ 0.69 (d, J_{PH} = 13.0 Hz, 9H), 0.73 (d, J = 6.6 Hz, 6H), 0.92 (d, J = 6.8 Hz, 6H), 1.10 (d, J = 6.7 Hz, 12H), 2.57 – 2.68 (m, 2H), 3.40 (sept, J = 6.6 Hz, 2H), 5.78 (dd, J = 7.9, 1.3 Hz, 2H), 6.53 (dd, J = 7.7, 1.4 Hz, 2H), 6.66 (td, J = 7.6, 1.4 Hz, 2H), 6.81 (td, J = 7.5, 1.3 Hz, 2H), 6.82 (s, 2H), 7.11 (dd, J = 16.9, 7.3 Hz, 6H). ^{1}H{^{31}P} NMR (C_6D_6, 400 MHz, 295K) δ 0.69 (s, 9H), 0.73 (d, J = 6.6 Hz, 6H), 0.92 (d, J = 6.8 Hz, 6H), 1.10 (d, J = 6.7 Hz, 12H), 2.57 – 2.68 (m, 2H), 3.40 (sept, J = 6.6 Hz, 2H), 5.78 (dd, J = 7.9, 1.3 Hz, 2H), 6.53 (dd, J = 7.7, 1.4 Hz, 2H), 6.66 (td, J = 7.6, 1.4 Hz, 2H), 6.81 (td, J = 7.5, 1.3 Hz, 2H), 6.82 (s, 2H), 7.11 (dd, J = 16.9, 7.3 Hz, 6H). ^{31}P{^{1}H} NMR (C_6D_6, 202 MHz, 295K) δ 70.88. ^{13}C{^{1}H} NMR (C_6D_6, 126 MHz, 295K) δ 15.76 (OP(CH_3)$_3$, d, J_{PC} = 69.3 Hz), 23.97 (^{i}Pr-CH_3), 25.20 (^{i}Pr-CH_3), 25.71 (^{i}Pr-CH_3), 29.21 (^{i}Pr-CH), 105.81 (Ar-CH), 114.04 (Ar-CH), 119.51 (Ar-CH), 122.69 (Ar-CH), 124.01 ($^{2,6\text{-iPr}}$Ar-CH), 125.50 ($^{2,6\text{-iPr}}$Ar-CH), 126.38 (im-CH), 126.40 (im-CH), 128.59 ($^{2,6\text{-iPr}}$Ar-CH), 142.51 (Ar-CN), 144.24 ($^{2,6\text{-iPr}}$Ar-C), 147.79 ($^{2,6\text{-iPr}}$Ar-C), 151.70 (Ar-CN).

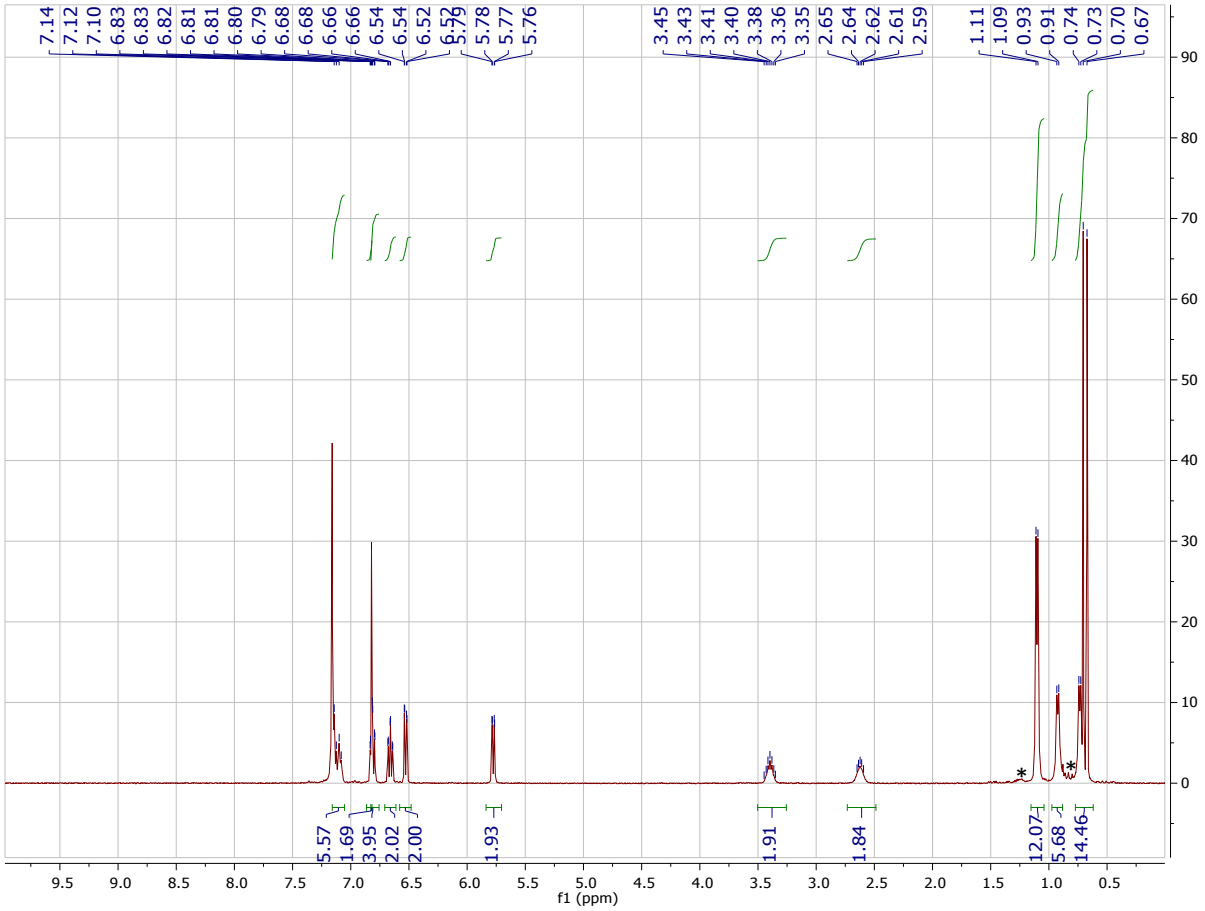

Fig. S17. ^{1}H NMR spectrum of Ti(dadi)OPMe$_3$ (**1**-OPMe$_3$); C_6D_6, 400 MHz, 295K.* = trace pentane

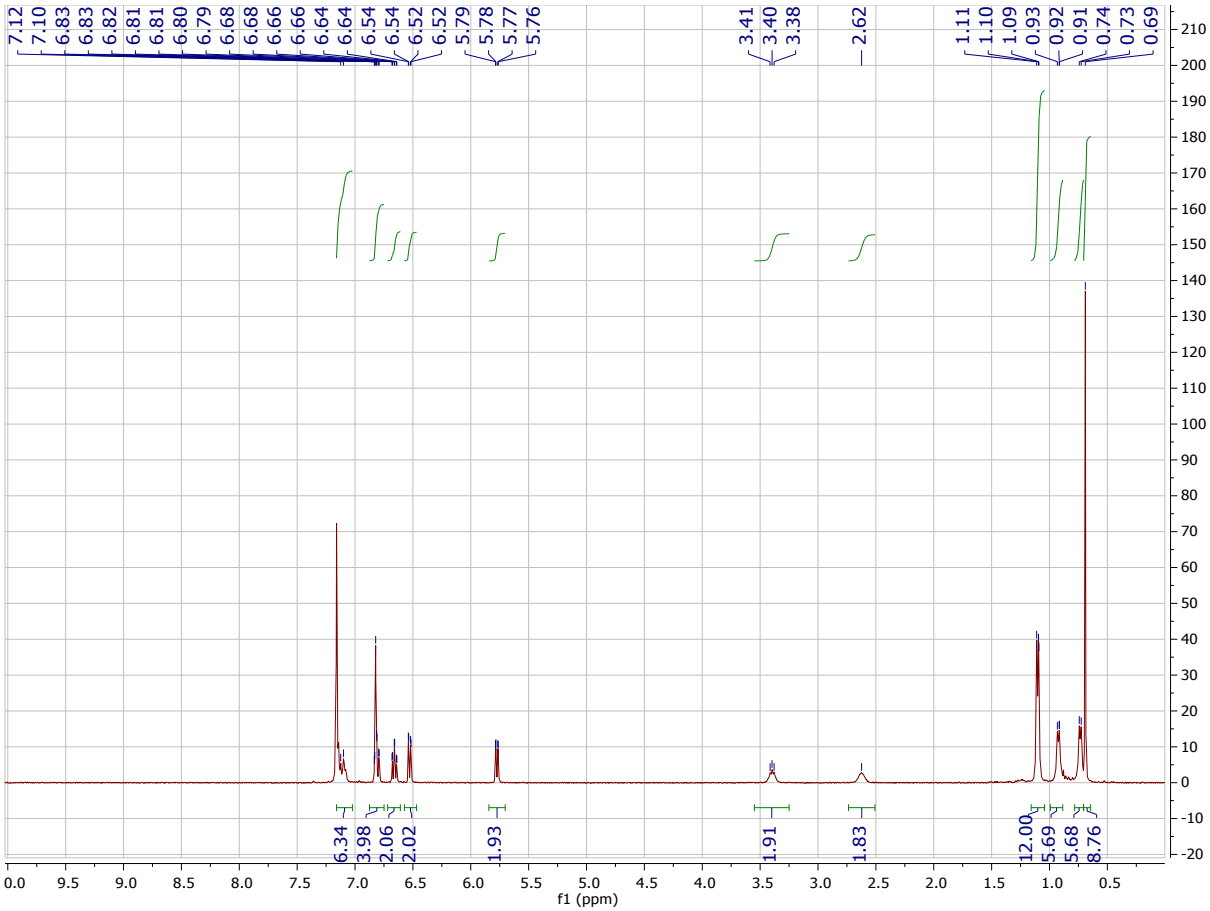

Fig. S18. $^{1}H\{^{31}P\}$ NMR spectrum of Ti(dadi)$OPMe_3$ (**1**-$OPMe_3$); C_6D_6, 400 MHz, 295K.

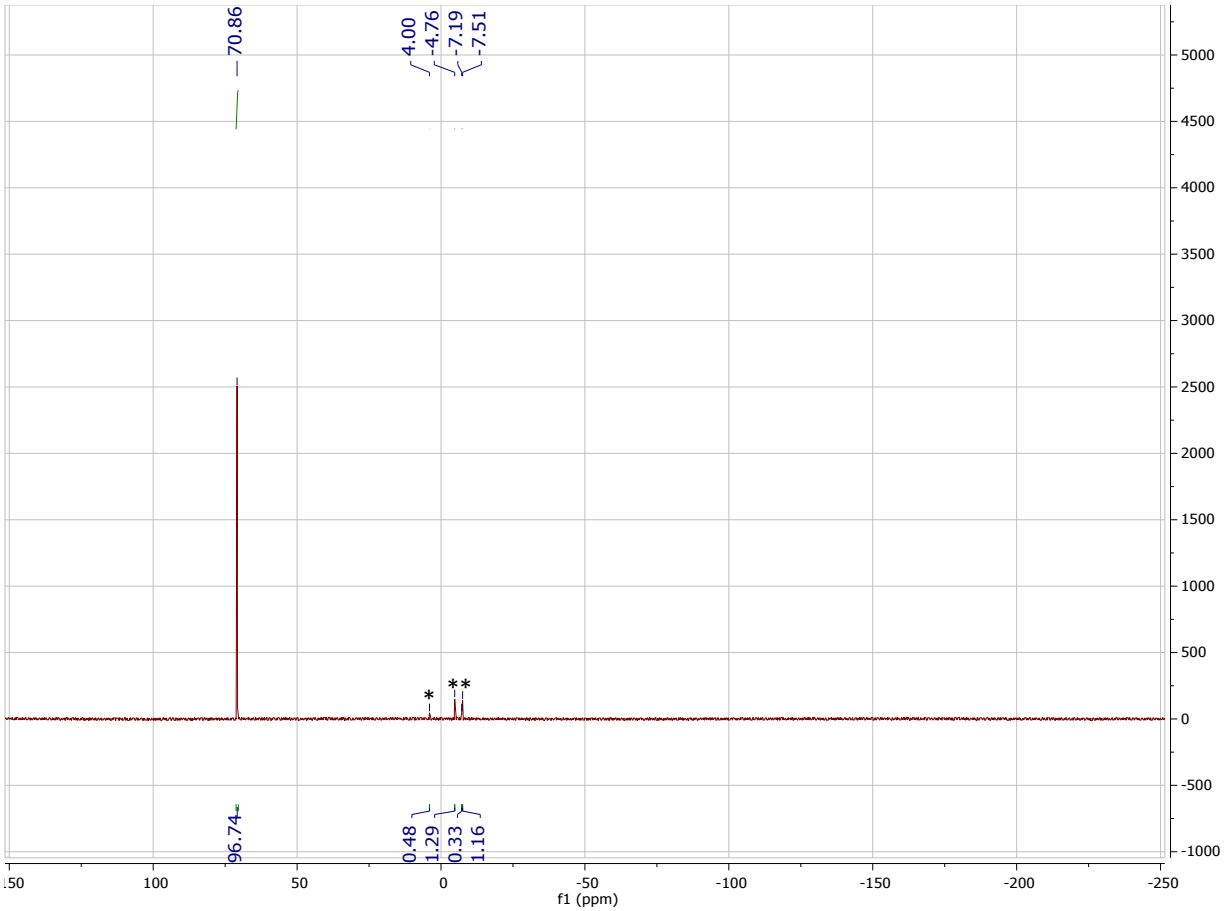

Fig. S19. ^{31}P NMR spectrum of Ti(dadi)$OPMe_3$ (**1**-$OPMe_3$); C_6D_6, 202 MHz, 295K, * = trace impurities

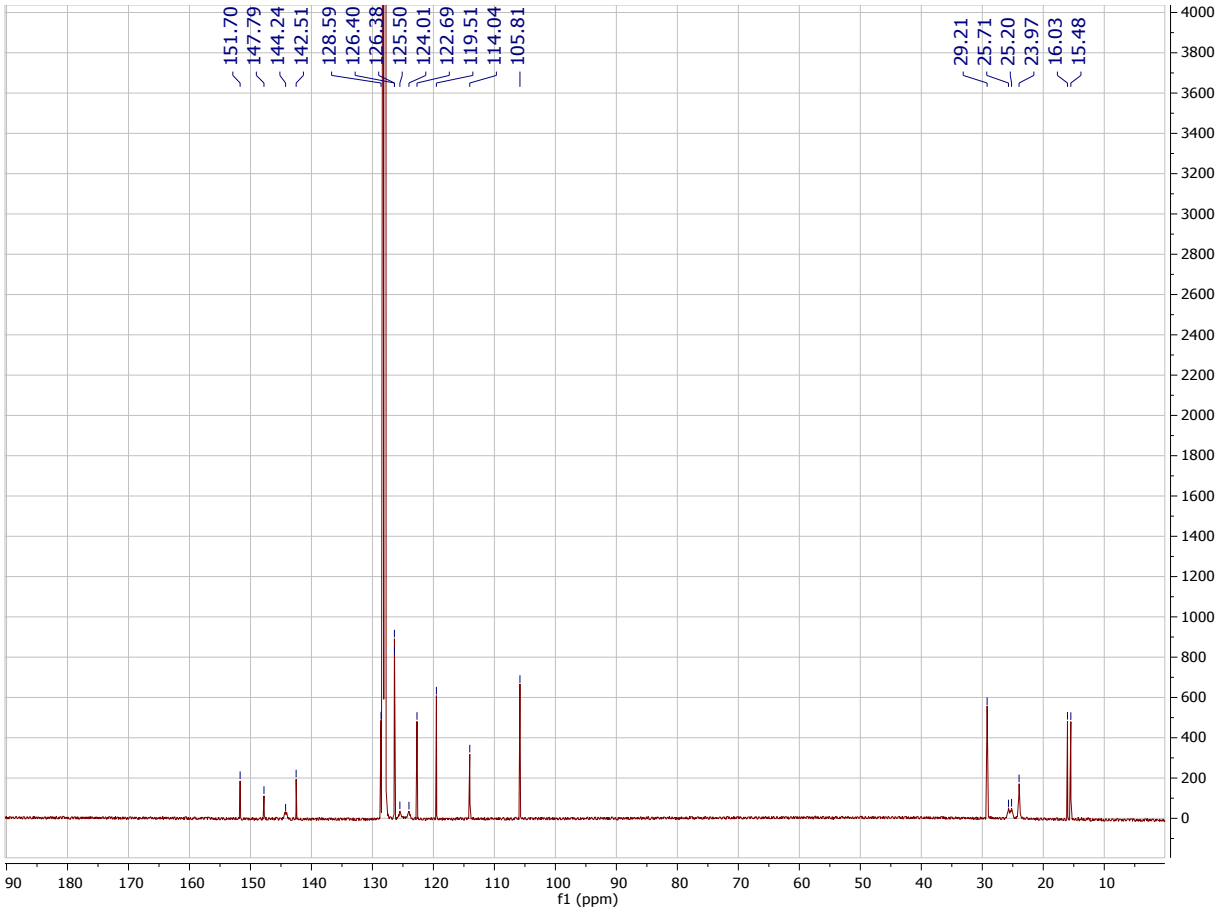

Fig. S20. $^{13}C\{^{1}H\}$ NMR spectrum of Ti(dadi)$OPMe_3$ (**1**-$OPMe_3$); C_6D_6, 126 MHz, 295K.

C. Procedure for Monitoring Carbonylation Reactions

The volumes of each NMR tube, sealed onto 14/20 ground glass joints and their designated needle valve adapter were determined by filling with water and measuring the mass. The tubes and needle valves were dried in an oven then charged with 0.5 mL of a stock solution of C_6D_6 containing 0.046 M Ti(dadi)NAd, *ca.* 0.40 M ferrocene, and 0.048 M THF in the dry box. These were then moved to the vacuum line on needle valve adapters. The NMR tubes were degassed with three freeze-pump-thaw cycles. 760 mm Hg of $CO_{(g)}$ was measured using a mercury monometer after being passed through a -78 ^{o}C trap. The needle valve was then closed and the tubes were cooled to 77 K with liquid nitrogen and flame-sealed with a CH_4/O_2 torch. The remaining gas in the headspace of the needle valve and 14/20 ground glass joint was measured using a Teopler pump. Each reaction was performed in triplicate at each temperature.

NMR tubes for catalytic carbonylation experiments were performed in the same fashion only with 600 mm Hg of $CO_{(g)}$ and using a stock solution containing $[Ti(dadi)NAd]_o$ = 0.0063 M, $[AdN_3]_o$ = 0.12 M, and *ca.* 0.005 M ferrocene.

II. Carbonylation Rate Analysis

Time dependent concentration plots obtained using ^{1}H NMR spectroscopy for catalytic runs were fit to a set of differential equations (eq. 1,2,3) describing the mechanistic model shown below (Scheme S1). Time dependent concentration plots obtained using ^{1}H NMR spectroscopy for stoichiometric runs were linearized then fitted in Microsoft Excel using linear regression. The Eyring plot was fitted in Igor Pro 6 using linear regression weighted by the standard deviation of each point. The standard deviation of each data point was determined using propagation of error calculations.[4] Carbon monoxide concentrations were calculated using the temperature dependent mole fraction solubility's (χ_g) extrapolated from reference 5 (Table S1).

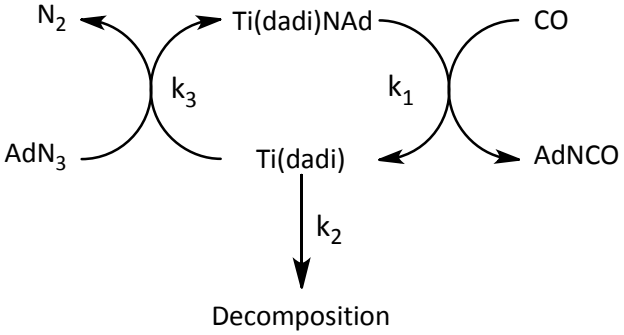

Scheme S1. Catalytic mechanism of carbonylation.

d[Ti(dadi)NAd]/dt = -k_1[TiNAd] + k_3[Ti(dadi)][AdN_3] (*eq*. 1)

d[Ti(dadi)]/dt = k_1[Ti(dadi)NAd] – k_2 – k_3[Ti(dadi)][AdN_3] (*eq*. 2)

d[AdN3]/dt = -k_3[Ti(dadi)][AdN_3] (*eq*. 3)

Where: $k_1 = k_{CO}$[CO]; k_3 = 1000 $M^{-1}s^{-1}$

P (atm)	T (K)	χ_g (at 1 atm)	[CO] at P
3.10	298± 0.1	6.59E-04	2.31E-02
3.21	308± 0.1	6.87E-04	2.49E-02
3.27	318± 0.1	7.12E-04	2.63E-02
3.34	328± 0.1	7.39E-04	2.79E-02
3.49	338± 0.1	7.73E-04	3.05E-02
3.60	348± 0.1	8.08E-04	3.29E-02

Table S1. Mole fraction solubility's (χ_g) of CO in benzene at 1 atm and specified temperature extrapolated from reference 5. Calculated [CO] (M) at the specified temperature and pressure.

Sample calculation of [CO] (M) at 3.1 atm and 298 K

Henry's Law: [5]

$P_g = \chi_g / H_T$ (*eq*. 4)

Where: P_g = partial pressure, χ_g = mole fraction solubility of gas dissolved, H_T = Henry's law constant at temperature T.

Mole fraction solubility of gas dissolved is:

$\chi_g = \eta_g / (\eta_g + \eta_s)$ (*eq*. 5)

Where: η_g = moles of gas and η_s= moles of solvent.

Henry's law constant at 298 K, and 1 atm:

$H_{298K} = (1 \pm 0.1 \text{ atm}) / (6.59 * 10^{-4} \pm 1.0 * 10^{-5}) = 1.52 * 10^3 \pm 38 \text{ atm}$

Mole fraction solubility of CO at the partial pressure in the reaction vessel (NMR tube):

$\chi_g = P / H_{298K} = (3.10 \pm 0.1 \text{ atm} / 1.52 * 10^3 \pm 38 \text{ atm}) = 2.04 * 10^{-3} \pm 1.2 * 10^{-4}$

Using equation 5 gives the moles of CO in 0.5 mL of C_6H_6:

$2.04 * 10^{-3} \pm 1.2 * 10^{-4} = \eta_{CO} / (\eta_{CO} + 5.61 * 10^{-3} \pm 1.3 * 10^{-5} \text{ mol } C_6H_6)$

$\eta_{CO} = 1.155 * 10^{-5} \pm 2.2 * 10^{-6}$ moles

Therefore:

$[CO] = (1.155 * 10^{-5} \pm 2.2 * 10^{-6} \text{ moles CO}) / (0.0005 \pm 1.1 * 10^{-7} \text{ L } C_6H_6) = 2.31 * 10^{-2} \pm 4.4 * 10^{-3} \text{ M}$

Catalytic carbonylation rate data and fits

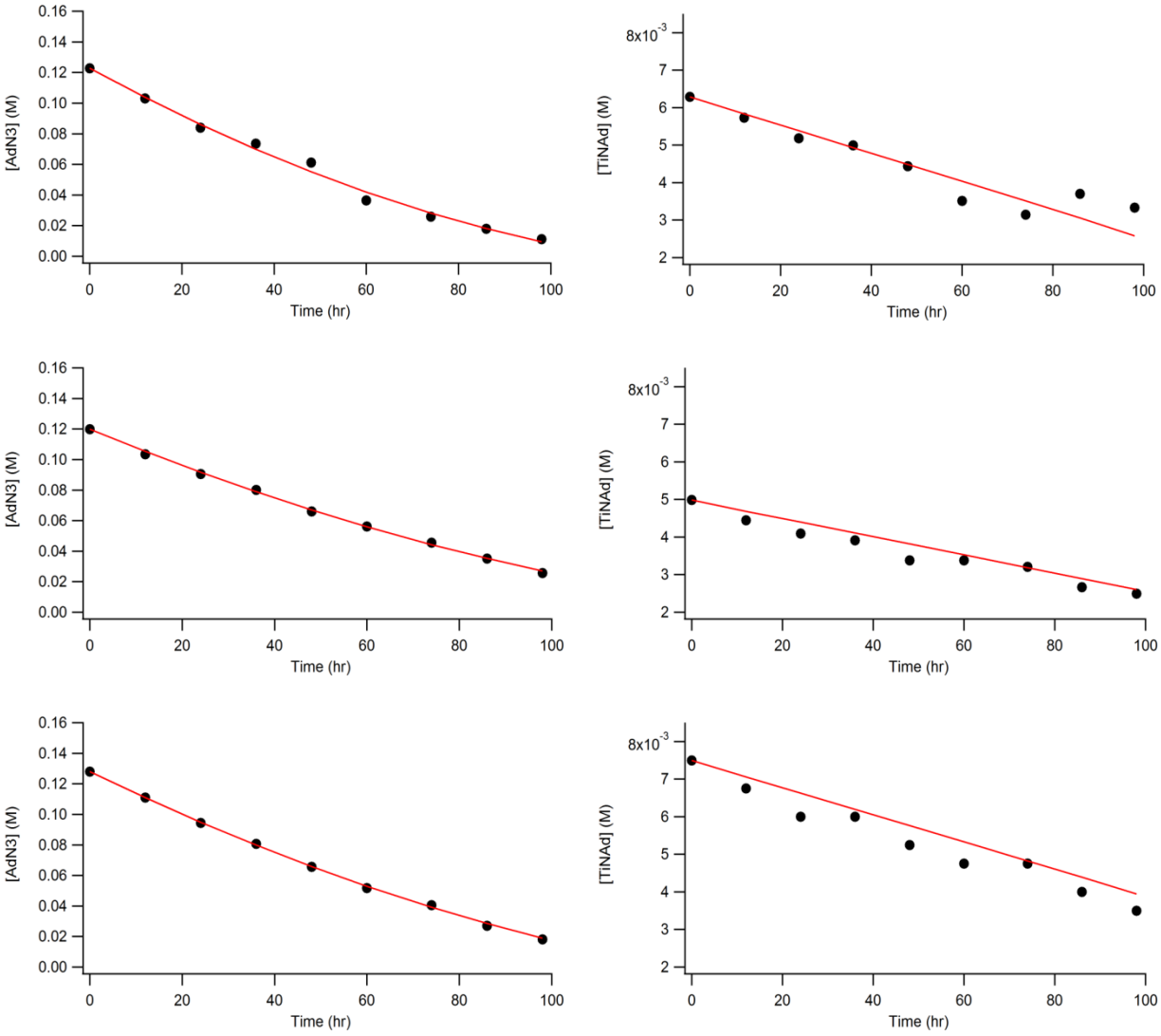

Fig. S21. Experimentally measured concentrations (black dots) and fitted data (red line) for catalytic carbonylation. Plots of [AdN_3] vs time (left) and [Ti(dadi)NAd] vs time (right). Run 1 (top), run 2 (middle), and run 3 (bottom). P_{CO} = 2.58 atm, [CO] = 0.022 M, $[Ti(dadi)NAd]_o$ = 0.0063 M, $[AdN_3]_o$ = 0.12 M, T = 298 K.

Run	k_{co} ($M^{-1}s^{-1}$)	k_{dec} (Ms^{-1})
1	$3.48*10^{-3} \pm 2.1*10^{-4}$	$3.70*10^{-5} \pm 6.2*10^{-6}$
2	$3.32*10^{-3} \pm 1.1*10^{-4}$	$2.38*10^{-5} \pm 3.0*10^{-6}$
3	$2.60*10^{-3} \pm 6.0*10^{-5}$	$3.53*10^{-5} \pm 3.1*10^{-6}$
Avg.	$3.13*10^{-3} \pm 2.4*10^{-4}$	$3.20*10^{-5} \pm 2.5*10^{-6}$

Table S2. Rate constants obtained from fits of experimental data for catalytic carbonylations.

Stoichimetric carbonylation rate data and analysis

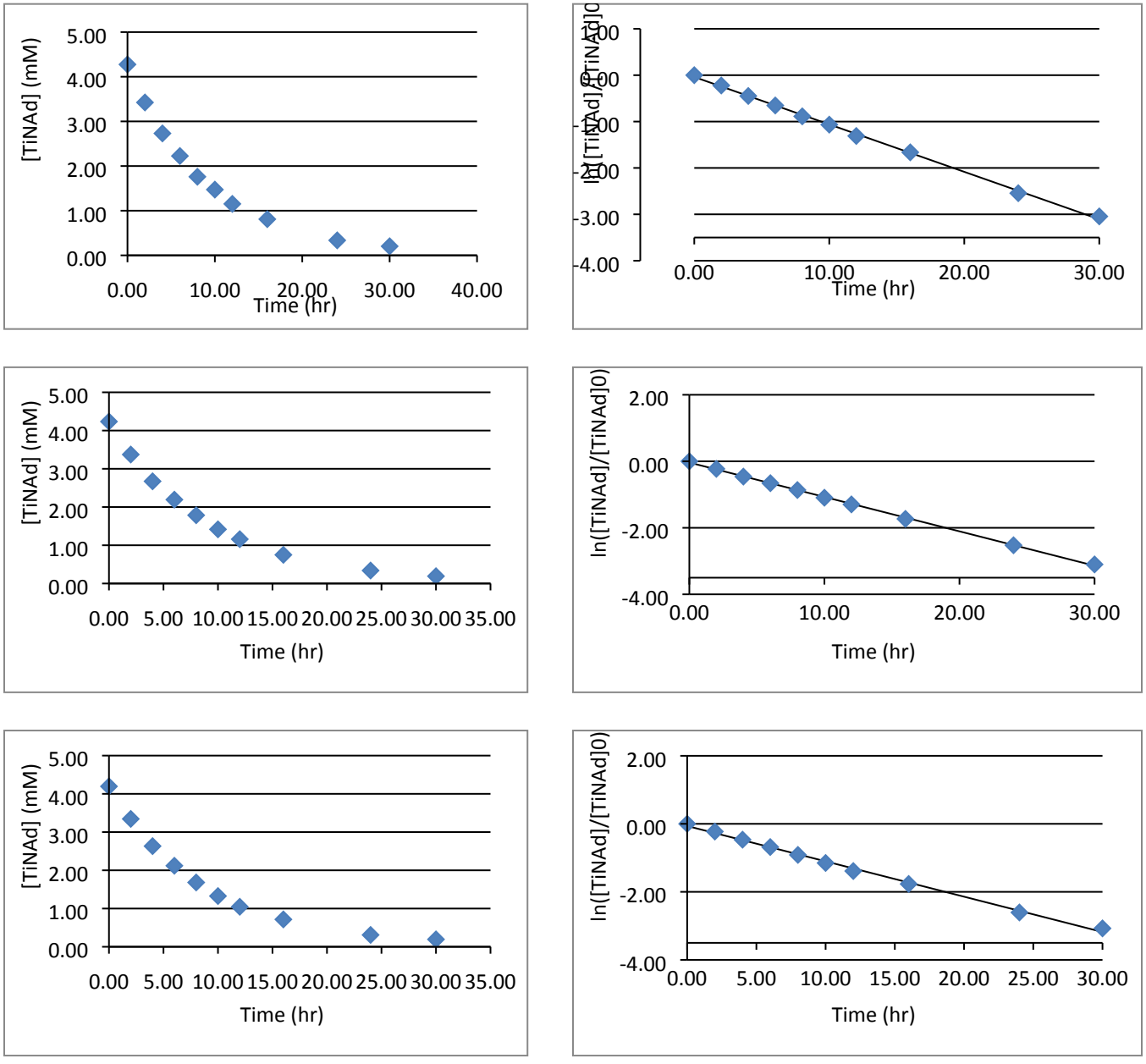

Fig. S22. Experimentally measured concentrations (blue diamonds) and fitted data (black line) for stoichiometric carbonylation. Run 1 (top), run 2 (middle), and run 3 (bottom). P_{CO} = 3.10 atm, [CO] = 0.023 M, $[TiNAd]_o$ = 0.047 M, $[THF]_o$ = 0.048 M, T = 298 K.

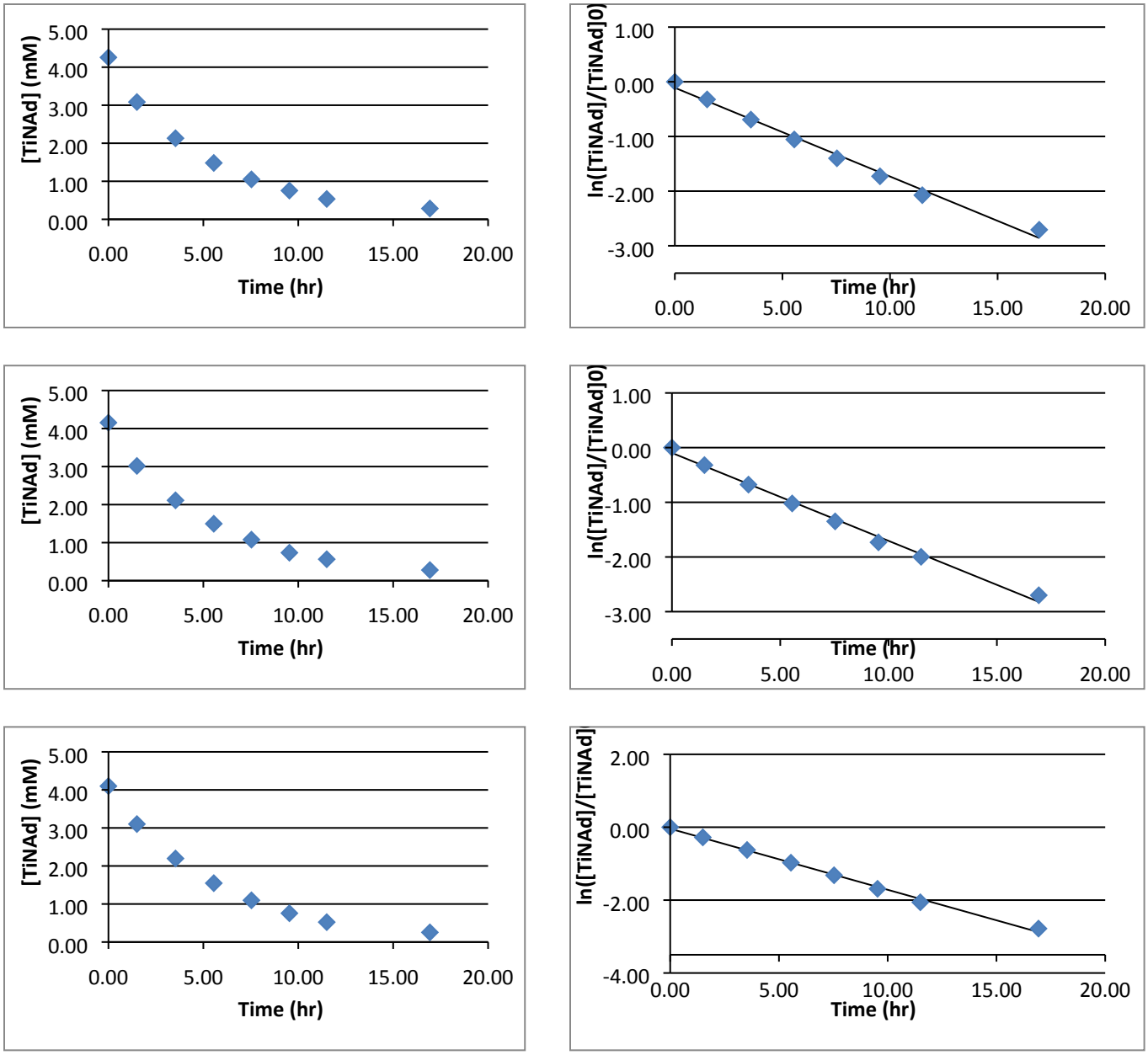

Fig. S23. Experimentally measured concentrations (blue diamonds) and fitted data (black line) for stoichiometric carbonylation at 308 K. Run 1 (top), run 2 (middle), and run 3 (bottom). P_{CO} = 3.21 atm, [CO] = 0.025 M, $[TiNAd]_o$ = 0.048 M, $[THF]_o$ = 0.048 M, T = 308 K.

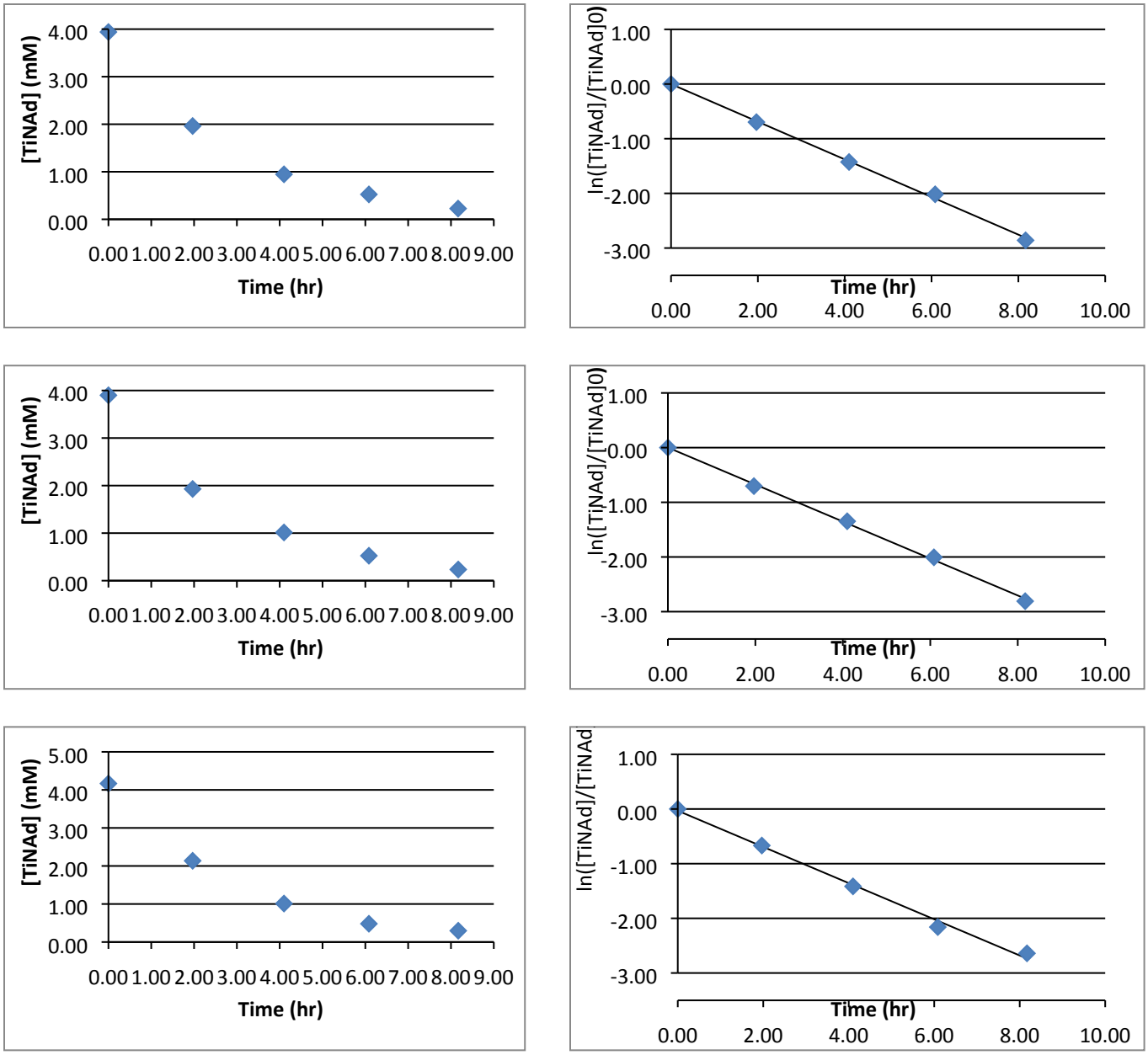

Fig. S24. Experimentally measured concentrations (blue diamonds) and fitted data (black line) for stoichiometric carbonylation at 318 K. Run 1 (top), run 2 (middle), and run 3 (bottom). P_{CO} = 3.27 atm, [CO] = 0.026 M, $[TiNAd]_o$ = 0.047 M, $[THF]_o$ = 0.048 M, T = 318 K.

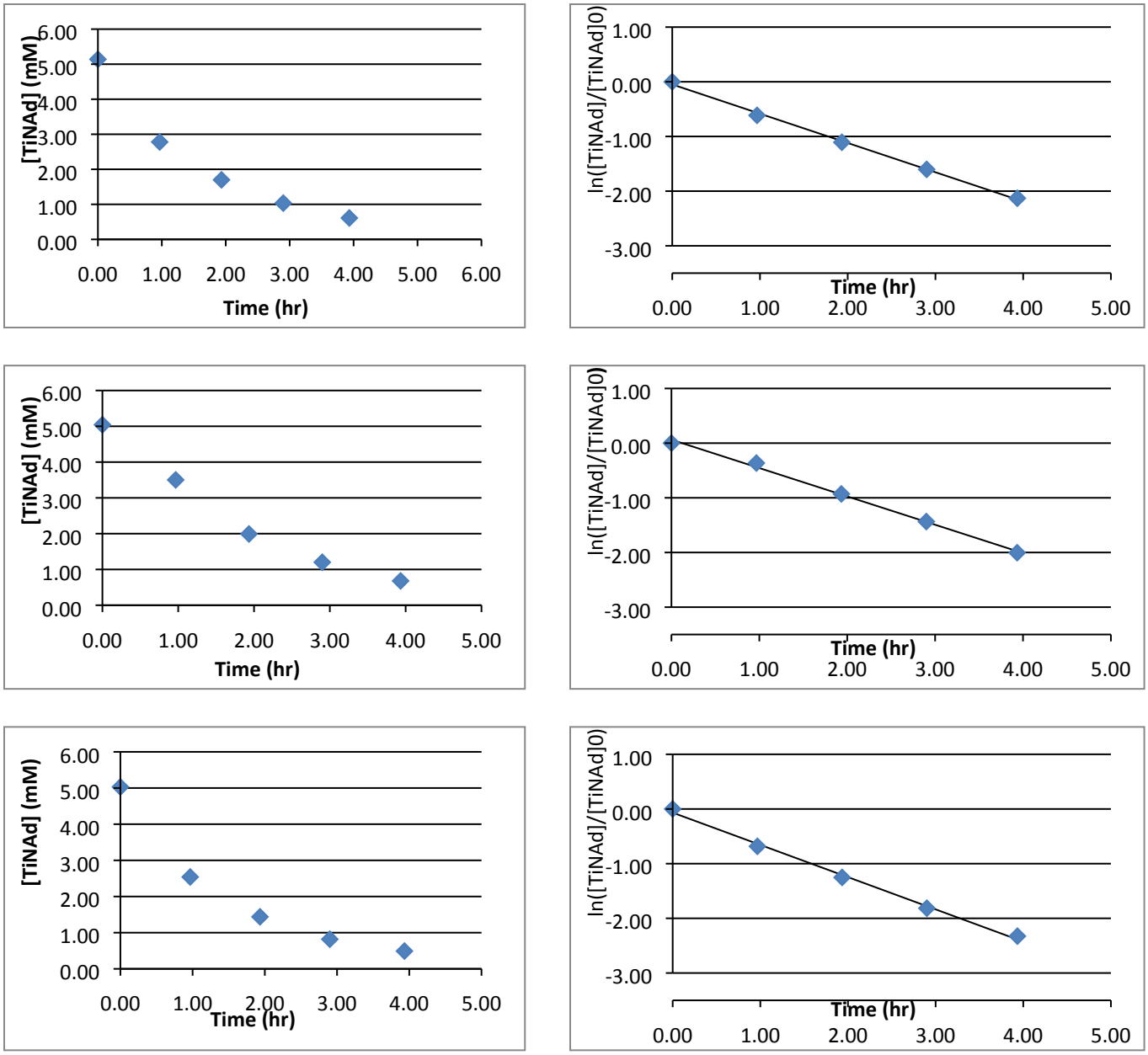

Fig. S25. Experimentally measured concentrations (blue diamonds) and fitted data (black line) for stoichiometric carbonylation at 328 K. Run 1 (top), run 2 (middle), and run 3 (bottom). P_{CO} = 3.34 atm, [CO] = 0.028 M, $[TiNAd]_o$ = 0.047 M, $[THF]_o$ = 0.048 M, T = 328 K.

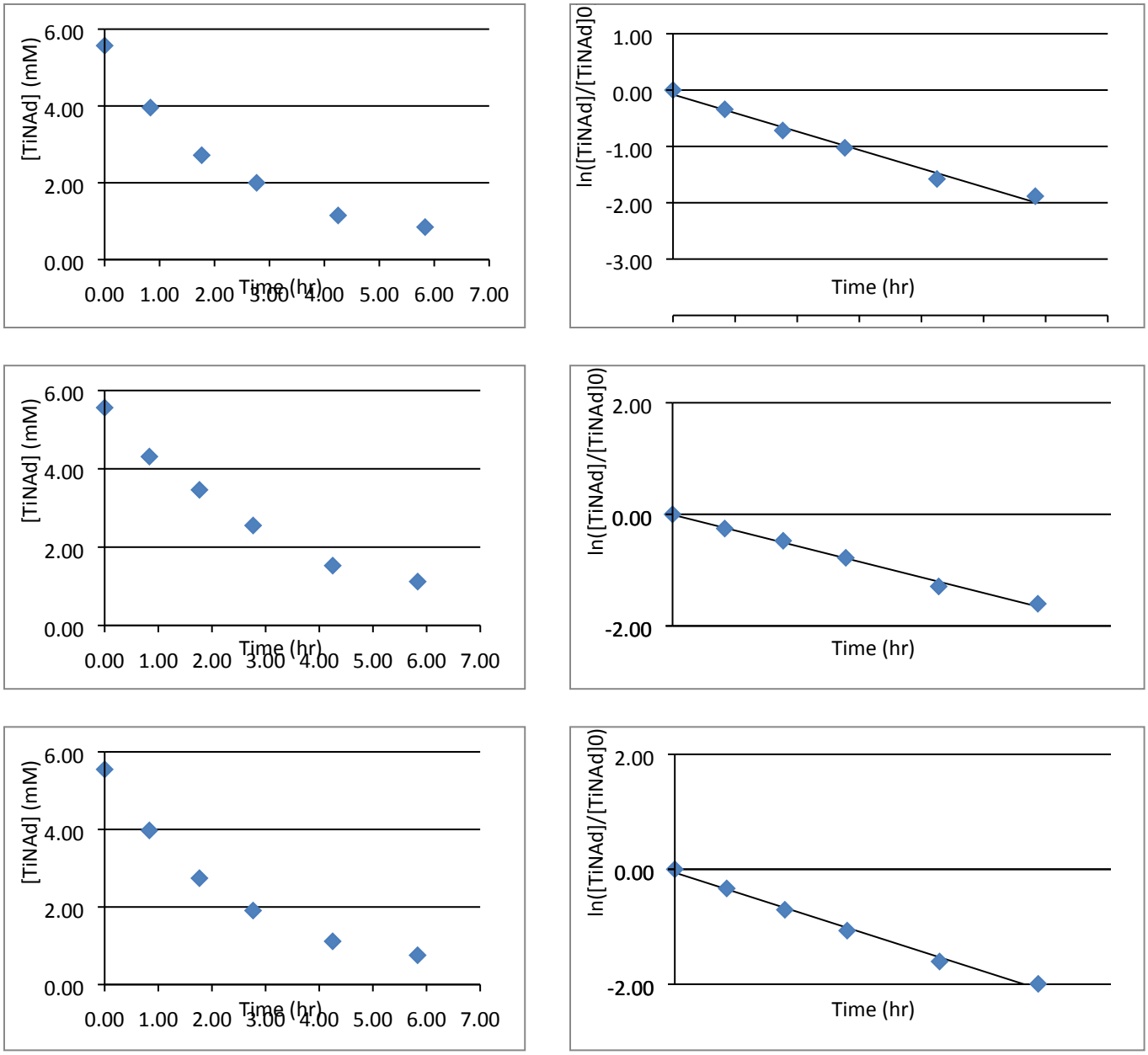

Fig. S26. Experimentally measured concentrations (blue diamonds) and fitted data (black line) for stoichiometric carbonylation at 338 K. Run 1 (top), run 2 (middle), and run 3 (bottom). P_{CO} = 3.49 atm, [CO] = 0.030 M, $[TiNAd]_o$ = 0.046 M, $[THF]_o$ = 0.048 M, T = 338 K.

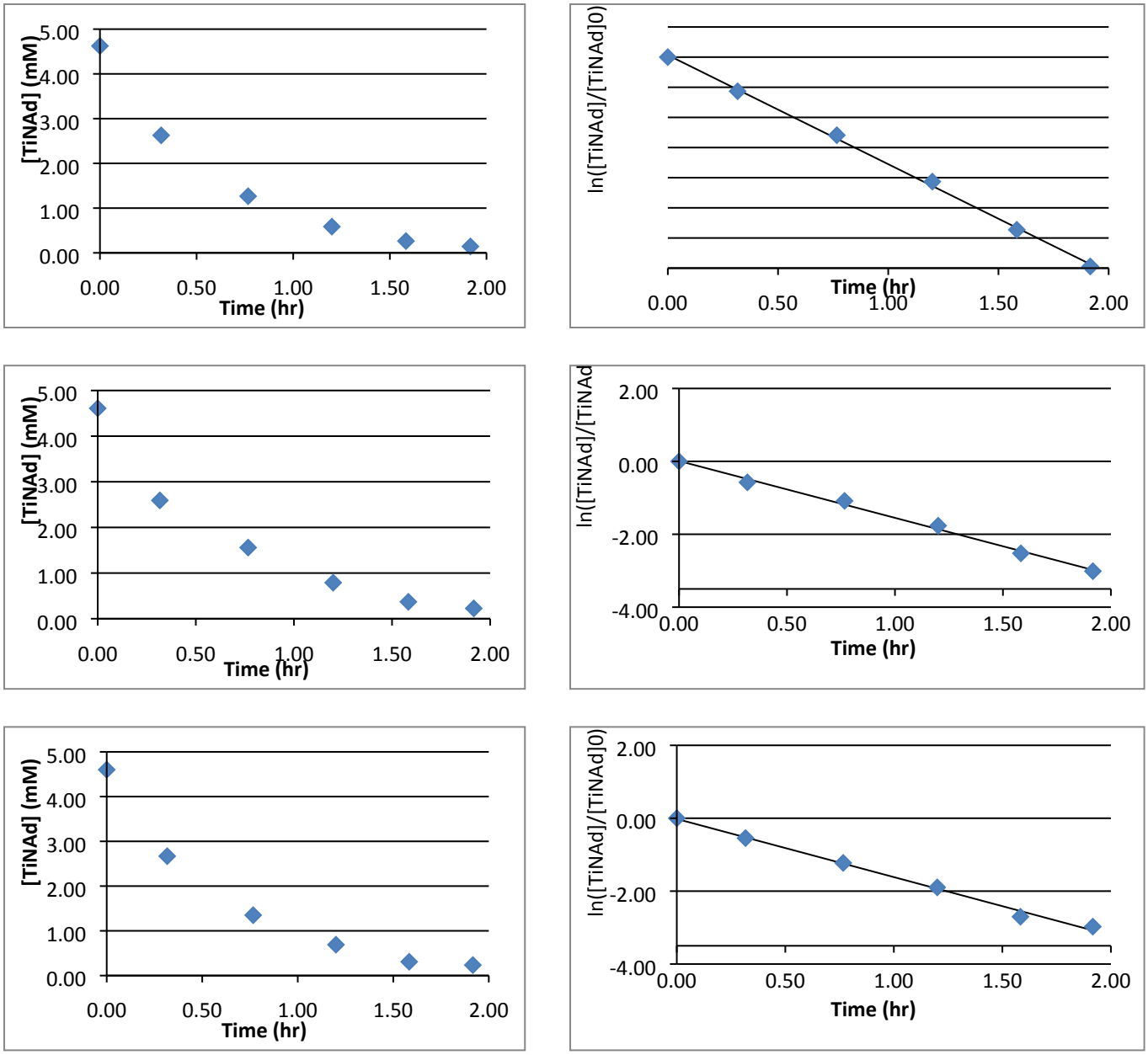

Fig. S27. Experimentally measured concentrations (blue diamonds) and fitted data (black line) for stoichiometric carbonylation at 348 K. Run 1 (top), run 2 (middle), and run 3 (bottom). P_{CO} = 3.60 atm, [CO] = 0.033 M, $[TiNAd]_o$ = 0.047 M, $[THF]_o$ = 0.048 M, T = 348 K.

Run	k_{co} (M^{-1} s^{-1}); 298 K	k_{co} (M^{-1} s^{-1}); 308 K	k_{co} (M^{-1} s^{-1}); 318 K	k_{co} (M^{-1} s^{-1}); 328 K	k_{co} (M^{-1} s^{-1}); 338 K	k_{co} (M^{-1} s^{-1}); 348 K
1	$1.24*10^{-3}$	$1.82*10^{-3}$	$3.65*10^{-3}$	$5.31*10^{-3}$	$8.55*10^{-3}$	$1.32*10^{-2}$
2	$1.25*10^{-3}$	$1.80*10^{-3}$	$3.59*10^{-3}$	$5.14*10^{-3}$	$7.25*10^{-3}$	$1.54*10^{-2}$
3	$1.26*10^{-3}$	$1.88*10^{-3}$	$3.51*10^{-3}$	$5.85*10^{-3}$	$8.04*10^{-3}$	$1.35*10^{-2}$
Avg.	$1.25*10^{-3}$	$1.83*10^{-3}$	$3.58*10^{-3}$	$5.44*10^{-3}$	$7.95*10^{-3}$	$1.40*10^{-2}$
σ	$5.50*10^{-5}$	$8.03*10^{-5}$	$1.49*10^{-4}$	$4.20*10^{-4}$	$8.57*10^{-4}$	$1.10*10^{-3}$

Table S3. Rate constants obtained from stoichiometric carbonylation reactions.

Eyring Analysis of Carbonylation:

T (°C)	k_{CO} (M^{-1} s^{-1})
25	$1.25*10^{-3} \pm 5.5*10^{-5}$
35	$1.83*10^{-3} \pm 8.0*10^{-5}$
45	$3.58*10^{-3} \pm 1.5*10^{-4}$
55	$5.44*10^{-3} \pm 4.2*10^{-4}$
65	$7.95*10^{-3} \pm 8.6*10^{-4}$
75	$1.40*10^{-2} \pm 1.1*10^{-3}$

Table S4. Rate constants with associated errors used for Eyring analysis.

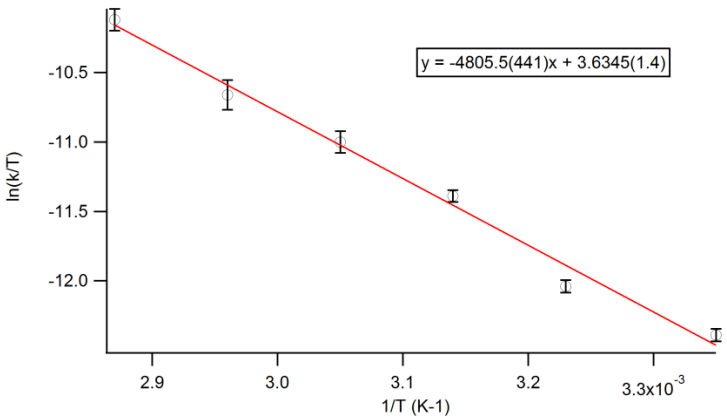

Fig. S28. Eyring plot for carbonylation. Experimentally determined rate constants (black circles) and linear regression weighted by standard deviation of each data point (red line).

slope	-4805.5 ± 441
intercept	3.6345 ± 1.4
$\Delta H^{‡}$ (kcal/mol)	9.6 ± 0.88
$\Delta S^{‡}$ (cal/mol)	-39.9 ± 2.78
$\Delta G^{‡}$ (kcal/mol) @ 55 °C	22.6 ± 0.90

Table S5. Activation parameters for carbonylation.

Determination of order in CO:

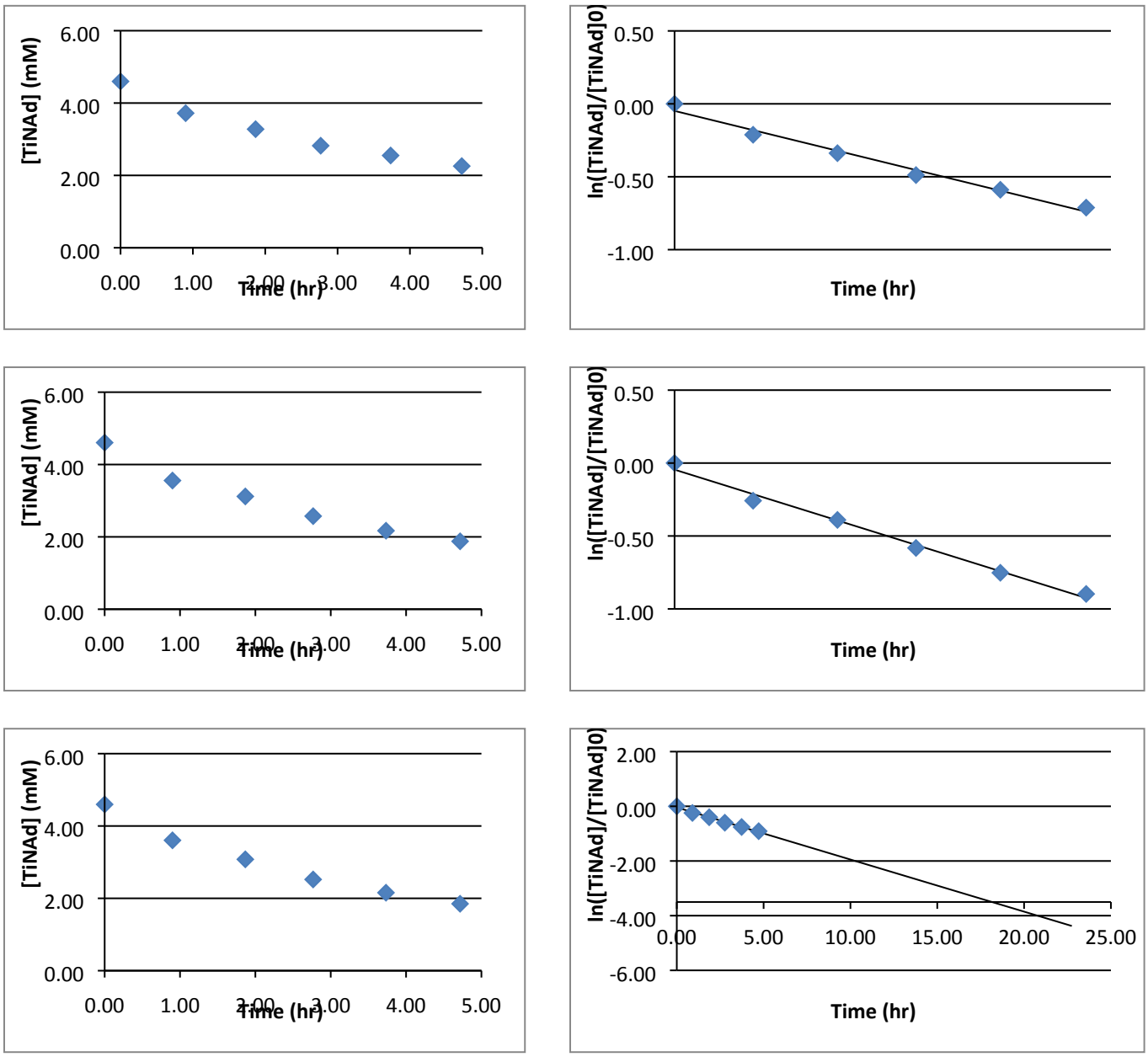

Fig. S30. Experimentally measured concentrations (blue diamonds) and fitted data (black line) for stoichiometric carbonylation at 328 K. Run 1 (top), run 2 (middle), and run 3 (bottom).). P_{CO} = 1.26 atm, [CO] = 0.015 M, $[TiNAd]_o$ = 0.047 M, $[THF]_o$ = 0.048 M, T = 328 K.

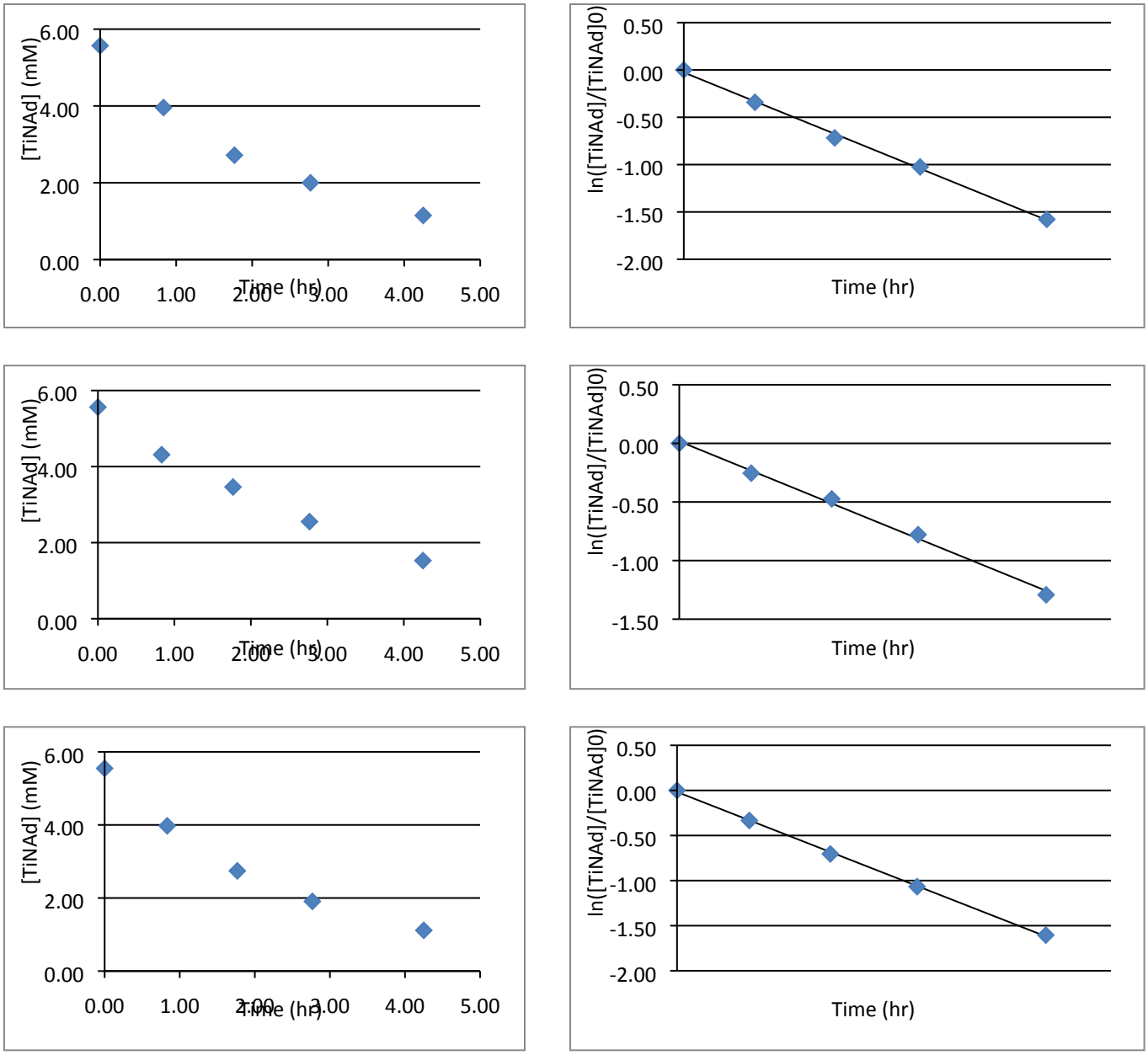

Figure S31: Experimentally measured concentrations (blue diamonds) and fitted data (black line) for stoichiometric carbonylation at 328 K. Run 1 (top), run 2 (middle), and run 3 (bottom). P_{CO} = 2.73 atm, [CO] = 0.023 M, $[TiNAd]_o$ = 0.046 M, $[THF]_o$ = 0.048 M, T = 328 K.

Run	k_{obs} (s^{-1}) [a]	k_{obs} (s^{-1}) [b]	k_{obs} (s^{-1}) [c]
1	$4.07*10^{-5}$	$1.02*10^{-4}$	$1.49*10^{-4}$
2	$5.18*10^{-5}$	$8.34*10^{-5}$	$1.44*10^{-4}$
3	$5.29*10^{-5}$	$1.05*10^{-4}$	$1.64*10^{-4}$
avg.	$4.85*10^{-5}$	$9.67*10^{-5}$	$1.52*10^{-4}$
σ	$5.53*10^{-6}$	$9.48*10^{-6}$	$1.04*10^{-5}$

Table S6: Observed rate constants for carbonylation. [a]P_{CO} = 1.26 atm, [CO] = 0.0105 M, $[TiNAd]_o$ = 0.047 M, $[THF]_o$ = 0.048 M, T = 328 K. [b]P_{CO} = 2.73 atm, [CO] = 0.023 M, $[TiNAd]_o$ = 0.046 M, T = 328 K. [c]P_{CO} = 3.34 atm, [CO] = 0.028 M, $[TiNAd]_o$ = 0.047 M, T = 328 K.

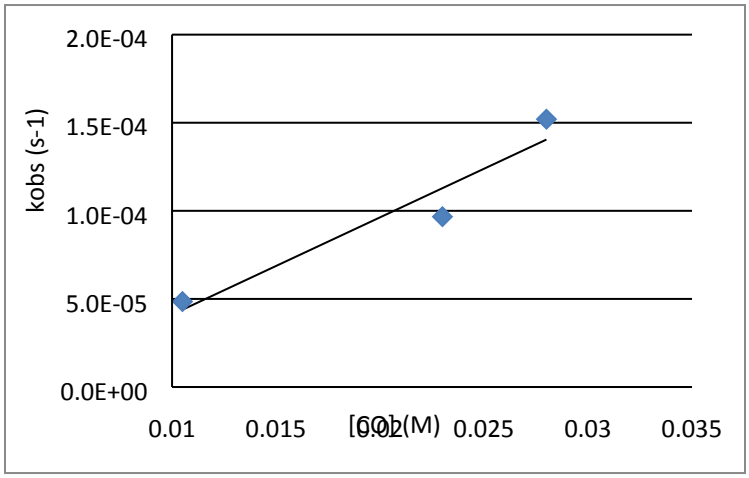

Figure S32: Plot of observed rate constant (k_{obs}) versus CO concentration. Experimentally determined observed rate constants (blue diamonds) and linear regression (black line) showing first order dependence on CO.

III. Computations

All simulations employed the Gaussian09[6] package. Geometries were optimized, and their energy Hessians computed to confirm them as either minima or transition states, at the ONIOM[7] (M06/6-311+G(d):UFF)[8,9] level of theory. Ultrafine integration grids were employed. The 2,6-$^{i}Pr_2$-Ar substituents were included in the UFF partition, and the remainder of the complex modeled with M06/6-311+G(d). For organic substrates, the alpha C of the 1-adamantyl substituent was included in the QM partition while the remainder was in the MM partition. Reported free energies for the transition metal complexes assume 1 atm and 298.15 K, except where noted, and were determined using unscaled vibrational frequencies.

Energies

M06/6-311+G(d) Calculated Enthalpies (H) and Free Energies (G), both in Hartrees, at 298.15 K and 1 atm. Spin states other than singlet are denoted by a superscripted prefix numeral.

Compound	**H**	**G**
N_2	-109.4816	-109.5033
CO	-113.2775	-113.3000
CO_2	-188.5437	-188.5679
N_2O	-184.6080	-184.6292
AdNC	-132.3482	-132.3884
AdN_3	-203.7020	-203.7446
AdNCO	-207.6132	-207.6572

THF	-232.2161	-232.2507
PMe_3	-460.8852	-460.9221
$OPMe_3$	-536.1287	-536.1678
Ti(dadi) (**1**)	-1607.9530	-1608.0612
^{3}Ti(dadi)	-1607.9520	-1608.0609
TiO(dadi) (**2**=O)	-1683.2248	-1683.3317
Ti(dadi)(NAd) (**2**=NAd)	-1702.2934	-1702.4125
Ti(dadi)(CO)	-1721.2720	-1721.3821
Ti(dadi)(□^{1}-N-AdNCO) (**1**-OCNAd)	-1815.6056	-1815.7268
Ti(dadi)(□^{1}-O-$OPMe_3$) (**1**-$OPMe_3$)	-2144.1662	-2144.2896
Ti(dadi)(THF) (**1**-THF)	-1840.2298	-1840.3451
Ti(dadi)(□^{1}-N-AdN_3) (**1**-N_3Ad)	-1811.7060	-1811.8274
Ti(dadi)(□^{1}-O-CO_2)	-1796.5198	-1796.6326
Ti(dadi)(CNAd)	-1740.3603	-1740.4848
TiO(dadi)(CNAd)	-1815.5943	-1815.6977

Geometries

ONIOM(M06/6-311+G(d):UFF) optimized singlet state of (dadi)Ti (**1**). Gray = C; blue = N; light gray = Ti. Hydrogen atoms omitted from the figure for clarity. Bond lengths in Å. Bond angles in °.

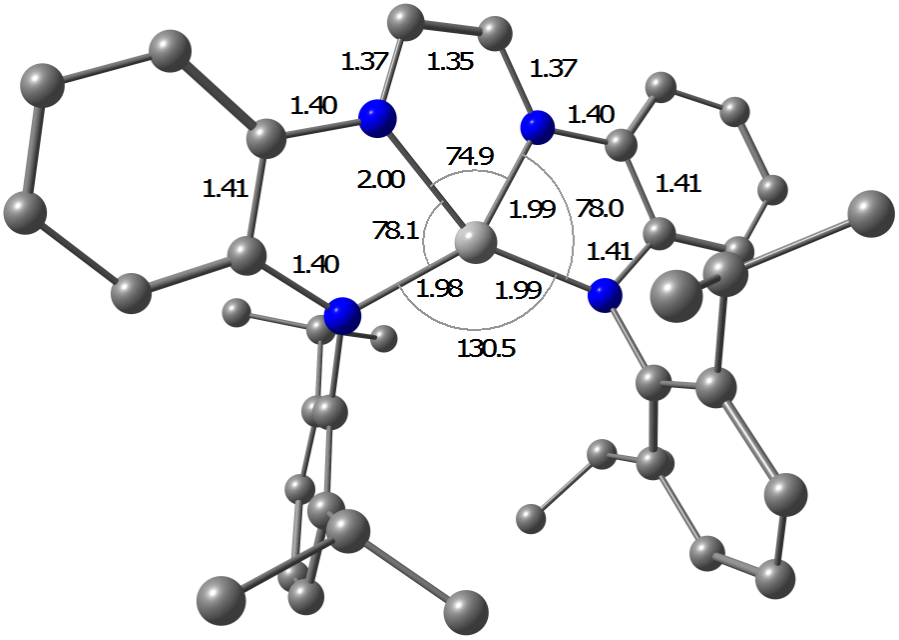

ONIOM(M06/6-311+G(d):UFF) optimized triplet state of (dadi)Ti (^{3}**1**). Gray = C; blue = N; light gray = Ti. Hydrogen atoms omitted from the figure for clarity. Bond lengths in Å. Bond angles in °.

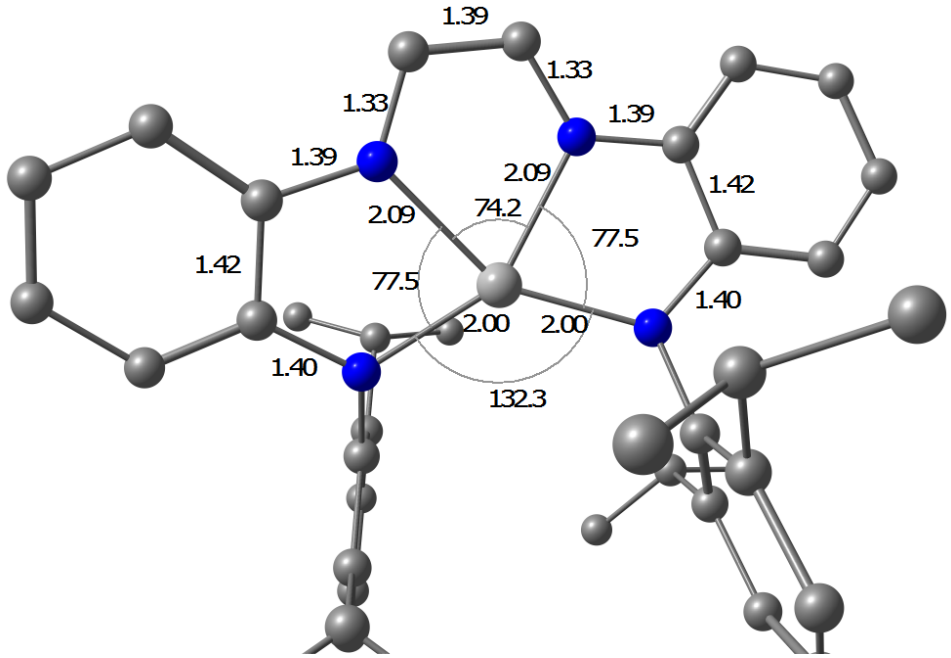

ONIOM(M06/6-311+G(d):UFF) optimized singlet ground state of (dadi)Ti(κ^1-N-N_3Ad). Gray = C; blue = N; light gray = Ti. Hydrogen atoms omitted from the figure for clarity. Bond lengths in Å. Bond angles in °.

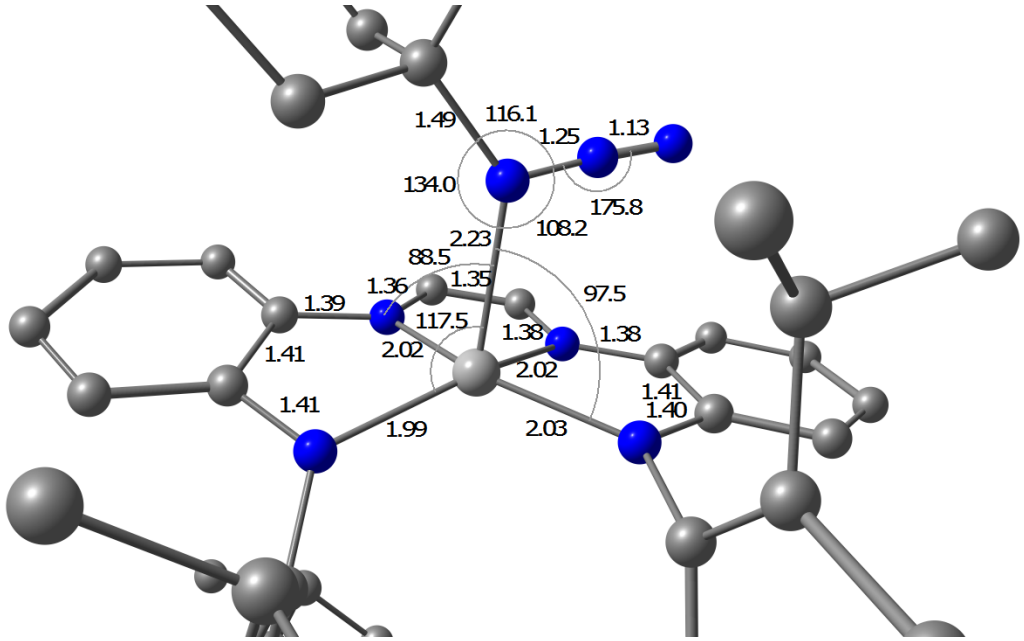

ONIOM(M06/6-311+G(d):UFF) optimized singlet ground state of (dadi)Ti(k1-AdNCO) (**1**-OCNAd). Gray = C; blue = N; O = red; light gray = Ti. Hydrogen atoms omitted from the figure for clarity. Bond lengths in Å. Bond angles in °.

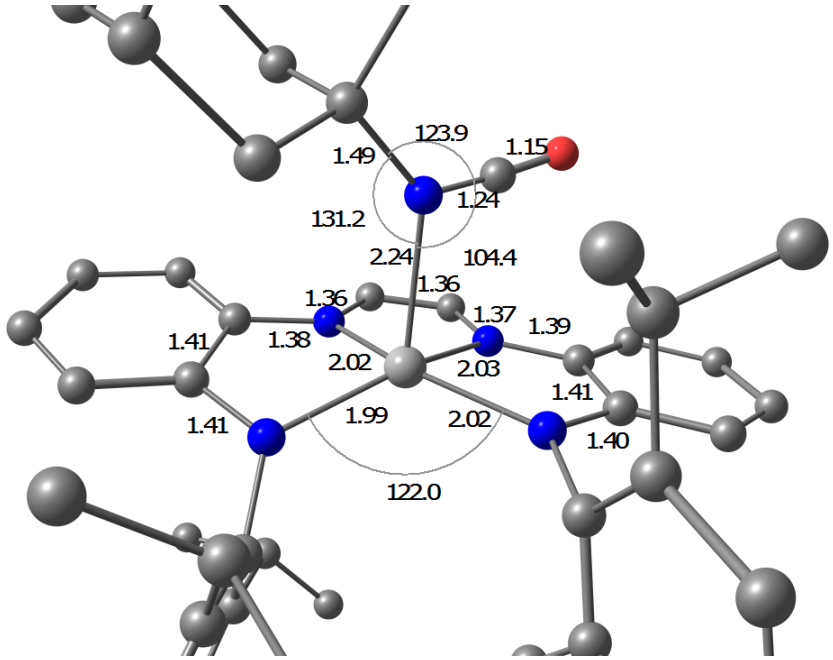

ONIOM(M06/6-311+G(d):UFF) optimized singlet ground state of (dadi)Ti=O (**2**=O). Gray = C; blue = N; O = red; light gray = Ti. Hydrogen atoms omitted from the figure for clarity. Bond lengths in Å. Bond angles in °.

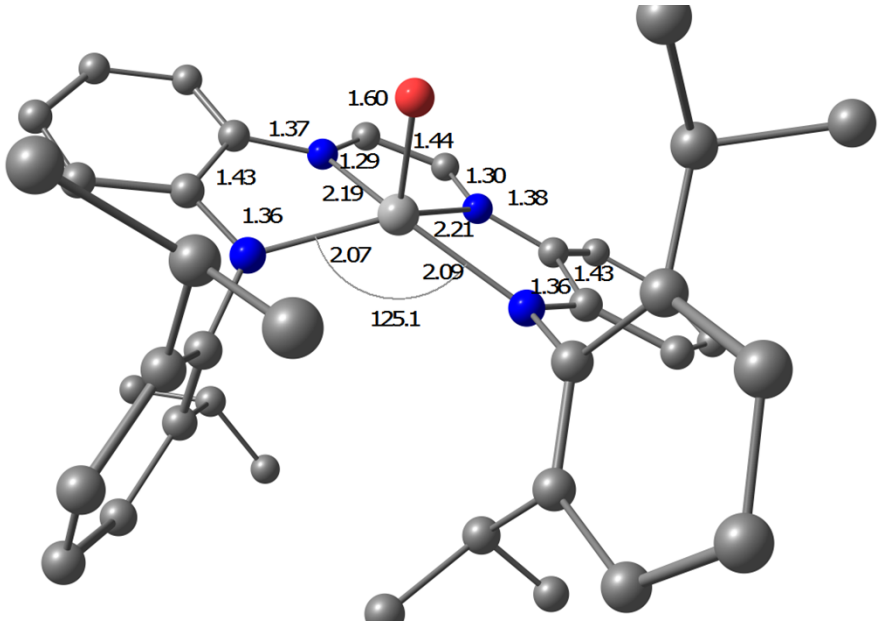

ONIOM(M06/6-311+G(d):UFF) optimized singlet ground state of (dadi)Ti=NAd (**2**=NAd). Gray = C; blue = N; light gray = Ti. Hydrogen atoms omitted from the figure for clarity. Bond lengths in Å. Bond angles in °.

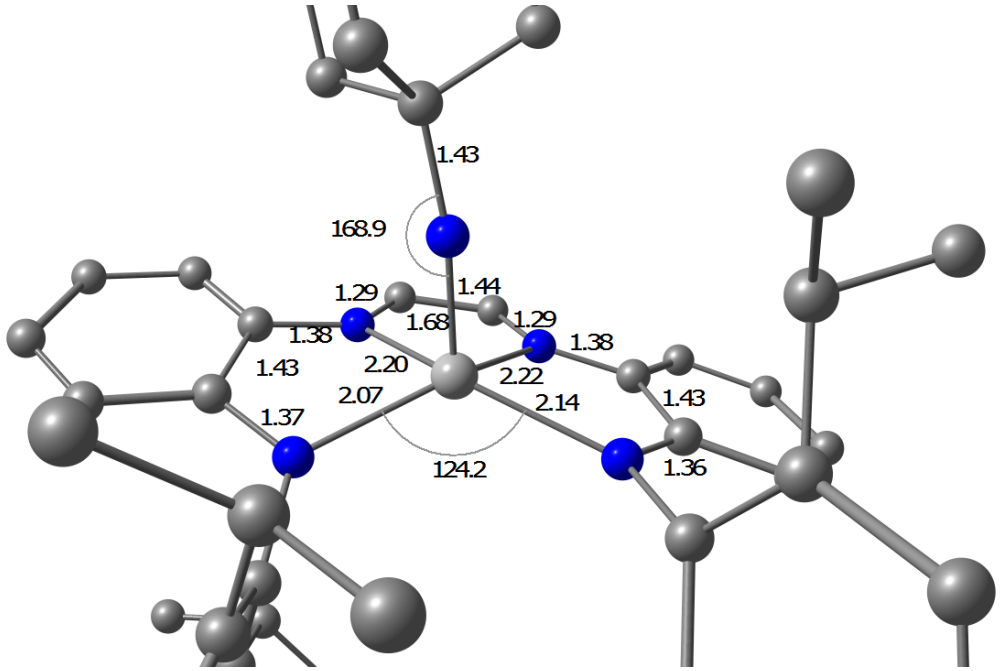

References:

1. S. P. Heins, W. D. Morris, P. T. Wolczanski, E. B. Lobkovsky, T. R. Cundari, *Angew. Chem. Int. Ed.* 2015, **54**, 14407-14411.

2. J. Eppinger, E. Herdtweck, R. Anwander, *Polyhedron*, 1998, **17**, 1195-1201.

3. J. J. H. Edema, R. Duchateau, S. Gambarotta, *Inorg. Chem.* 1991, **30**, 154-6.

4. J. R. Taylor, *An Introduction to Error Analysis: The Study of Uncertainties in Physical Measurements*; *2nd Ed.;* University Science Books: Sausalito, 1997.

5. P. G. T. Fogg, W. Gerrard, *Solubility of Gases in Liquids*; John Wiley & Sons: Chichester, 1991, Ch.1, 3, 13.

6. M. J. Frisch, G. W. Trucks, H. B. Schlegel, G. E. Scuseria, M. A. Robb, J. R. Cheeseman, G. Scalmani, V. Barone, B. Mennucci, G. A. Petersson, H. Nakatsuji, M. Caricato, X. Li, H. P. Hratchian, A. F. Izmaylov, J. Bloino, G. Zheng, J. L. Sonnenberg, M. Hada, M. Ehara, K. Toyota, R. Fukuda, J. Hasegawa, M. Ishida, T. Nakajima, Y. Honda, O. Kitao, H. Nakai, T. Vreven, J. A. Montgomery Jr., J. E. Peralta, F. Ogliaro, M. J. Bearpark, J. Heyd, E. N. Brothers, K. N. Kudin, V. N. Staroverov, R. Kobayashi, J. Normand, K. Raghavachari, A. P. Rendell, J. C. Burant, S. S. Iyengar, J. Tomasi, M. Cossi, N. Rega, N. J. Millam, M. Klene, J. E. Knox, J. B. Cross, V. Bakken, C. Adamo, J. Jaramillo, R. Gomperts, R. E. Stratmann, O. Yazyev, A. J. Austin, R. Cammi, C. Pomelli, J. W. Ochterski, R. L. Martin, K. Morokuma, V. G. Zakrzewski, G. A. Voth, P. Salvador, J. J. Dannenberg, S. Dapprich, A. D. Daniels, Ö. Farkas, J. B. Foresman, J. V. Ortiz, J. Cioslowski, D. J. Fox, Gaussian, Inc., Wallingford, CT, USA, **2009**.

7. M. Svensson, S. Humbel, R. D. J. Froese, T. Matsubara, S. Sieber, K. Morokuma, *J. Phys. Chem.* **1996**, *100*, 19357-19363.

8. Y. Zhao, D. G. Truhlar, *Theor. Chem. Acc.* 2008, **120**, 215-241.

9. A. K. Rappe, C. J. Casewit, K. S. Colwell, W. A. Goddard, III, W. M. Skiff, *J. Am. Chem. Soc.* 1992, **114**, 10024-10035.